



Epidemiological Viability and Control of Rotavirus: A Mathematical Modelling Approach

^{*1}Loyinmi, A.C., & ²Gbodogbe, S.O.

¹Department of Mathematics, Tai Solarin University of Education, Ogun State, Nigeria

²Department of Mathematical Science, University of Indianapolis, Indiana, USA

*Corresponding author email: loyinmiac@tasued.edu.ng

Abstract

To effectively address rotavirus infections, interventions must be tailored to specific socio-economic contexts and target populations. This study presents a mathematical model to describe the dynamics of rotavirus, emphasizing the importance of a comprehensive approach to combating the infection. Sensitivity analysis reveals the influence of each variable on disease spread and assesses the model's robustness across different parameter values. The model's epidemiological viability is demonstrated by its equilibrium in endemic conditions, stability in disease-free scenarios, non-negativity, and boundedness. Optimal control measures significantly impact virus transmission, with simulations showing that combining diverse strategies effectively reduces the spread of rotavirus. These findings highlight the importance of balanced and adaptable control measures, leading to enhanced immunity, reduced infection rates, and better health outcomes for affected communities.

Keywords: Mathematical Model, Rotavirus, Sensitivity Analysis, Optimal control, Epidemiological viability

Introduction

Ruth Bishop and colleagues used electron micrography to find a viral particle in the intestinal mucosa of infants who had diarrhoea in 1973. The name "rotavirus" was given to this virus as a result of its resemblance to a wheel (*rota* is Latin for wheel) (Margaret & Penina., 2021). Before the introduction of vaccines, it is estimated that around 2.7 million cases of rotavirus infections occurred annually in the United States. Approximately 95% of children had at least one rotavirus infection by the age of 5 years. These infections led to significant healthcare burdens, including 410,000 physician visits, over 200,000 emergency department visits, 55,000 to 70,000 hospitalizations, and 20 to 60 deaths each year in children under the age of 5. Rotavirus was responsible for 30% to 50% of all hospitalizations due to gastroenteritis in this age group, with the highest incidence of clinical illness observed among children aged 3 to 35 months (Margaret et al., 2021; Loyinmi et al., 2021; Ilmi et al., 2020). As of 2016, rotavirus continued to be the primary cause of fatal diarrhea in children globally, resulting in nearly 129,000 deaths in children aged 5 and under. Approximately half of these fatalities were concentrated in four nations: the Democratic Republic of the Congo, India, Nigeria, and Pakistan (Sydney, 2023; Agbomola & Loyinmi, 2022b). Rotavirus is a global presence, with its occurrence spanning across the world. Before the introduction of vaccines, the share of severe diarrhea cases in children under the age of 5 attributed to rotavirus was comparable, approximately 35% to 40%, in both developed and developing nations. This suggests that solely enhancing sanitation measures is insufficient for infection prevention. Additionally, the prevalence of distinct rotavirus genotypes can vary based on geographical location and time period (Margaret & Penina., 2021). The rotavirus is frequently transmitted through hand-to-mouth contact, and infection can occur when you touch a contaminated object or surface and subsequently touch your mouth. Another route of infection is through the consumption of contaminated food. The virus is shed through feces, and according to the CDC, this is how it enters the environment. The majority of infections occur when individuals come into contact with infected fecal matter (Margaret et al., 2021; Sydney, 2023; Agbomola & Loyinmi, 2022b). To prevent the spread of rotavirus, it is important to practice thorough hand washing after handling and disposing of a child's soiled diaper. Additionally, it's advisable to disinfect areas used for food preparation or consumption, as well as surfaces that may have been in contact with stool or urine during diaper changes (Idowu & Loyinmi, 2023a; Loyinmi et al., 2023; Pitzer et al., 2012).

Mathematical modelling has serves as a crucial tool for public health decision-makers and researchers (Loyinmi & Ijaola, 2024a; Loyinmi & Ijaola, 2024b; Loyinmi et al., 2024; Idowu & Loyinmi, 2023b). It has empowers them

to gain a deeper understanding of disease dynamics, develop effective strategies for disease control and prevention, allocate resources efficiently, and ultimately improve the health and well-being of communities (Loyinmi & Gbodogbe, 2024; Kraay et al., 2018). This interdisciplinary approach plays a vital role in addressing diseases like rotavirus and other public health challenges worldwide (Lee et al., 2024; De Blasio et al., 2010)

Since the introduction of the rotavirus vaccine, dynamic mathematical models have played a crucial role in assessing its impact on severe rotavirus-related deaths and the overall prevalence of diarrhoea in diverse socio-economic contexts (Loyinmi et al., 2024; Ernest et al., 2020; Park et al., 2017; Pitzer et al., 2012). These modelling studies have examined the factors driving the transmission dynamics of rotavirus within countries, identified critical elements influencing vaccine effectiveness, and proposed strategies to enhance its efficacy. Notably, it has been demonstrated that the failure to complete the recommended vaccine schedule can significantly diminish its effectiveness (Gbodogbe, 2025; Darti et al., 2020; Lopman et al., 2012; De Blasio et al., 2010; Shim & Galvani, 2009). However, it's important to recognize that while rotavirus vaccines have proven highly effective, there has been insufficient attention given to alternative methods of controlling rotavirus. While vaccines have been a key component, a comprehensive approach to rotavirus control should encompass a combination of vaccination and other preventive measures. These measures include promoting better hygiene practices, advocating for breastfeeding, utilizing oral rehydration therapy (ORT), providing zinc supplementation, and strengthening healthcare systems (Sydney, 2023; Agbomola & Loyinmi, 2022a; Margaret et al., 2021; Gaalen et al., 2017; Shim & Galvani, 2009; White et al, 2008). To achieve a holistic approach to tackling rotavirus infections, interventions must be tailored to specific socio-economic contexts and target populations. This research paper emphasizes the importance of such a comprehensive strategy to address rotavirus infections comprehensively.

Materials and Methods

We adapted and modified a model similar to the SIRS (Susceptible-Infectious-Recovered-Susceptible) model developed by Ernest O. and colleagues (Ernest et al, 2020). In brief, the model includes the following classes: Maternal (M): Represents individuals with maternal immunity that gradually diminishes over time, making them fully susceptible to the initial infection (S_0). Vaccinated before first infection (V_0): Represents individuals who received a rotavirus vaccine before experiencing their first infection. First infection (I_1): Represents individuals in the early stages of their first rotavirus infection. Severe cases of first infection requiring hospitalization (H_1). Recovered from the first infection (R_1): Represents individuals who have recovered from their first infection but may still be susceptible to subsequent infections. Susceptible to secondary infection (S_1): Individuals in this class have lost immunity gained from the first infection and are now susceptible to a secondary infection. Vaccinated before second infection (V_1): Represents individuals who received a rotavirus vaccine before their second infection. Second infection (I_2): Represents individuals experiencing a second rotavirus infection, with assumed lower infectiousness compared to the first infection. Severe cases of second infection requiring hospitalization (H_2). Recovered from the second infection (R_2): Represents individuals who have recovered from their second infection but may still have temporary immunity. Partially immune susceptible to subsequent infections (S_2): Individuals in this class have temporary immunity after the second infection, which gradually wanes over time, making them susceptible to subsequent infections, typically milder or asymptomatic. Vaccinated before third infection and subsequent infection (V_3): Represents individuals who received a rotavirus vaccine before their third infection and subsequent infection. Third infection and subsequent infection (I_3): Represents individuals experiencing a third rotavirus infection and subsequent infection, with assumed lower infectiousness compared to previous infections. Severe cases of third infection and subsequent infection requiring hospitalization (H_3). Recovered from the third infection and subsequent infection (R_3): Represents individuals who have recovered from their third infection and subsequent infection but may still have temporary immunity. After the temporary immunity wanes, individuals return to the partially-immune susceptible class (S_2) and remain subject to subsequent infections. This model allows for a detailed exploration of the dynamics of rotavirus infection, vaccination, hospitalization and immunity over multiple infection cycles.

The force of rotavirus infection is given as

$$\Lambda = \Phi(I_1 + \theta_1 M + \theta_2 V_0 + \theta_3 H_1 + \theta_4 V_1 + \theta_5 I_2 + \theta_6 H_2 + \theta_7 V_2 + \theta_8 I_3 + \theta_9 H_3) \quad (1)$$

Where Φ denotes rotavirus contact rate, θ_2, θ_5 , and θ_8 represent the adjustment rate infectious state and $\theta_1, \theta_3, \theta_4, \theta_6, \theta_7$ and θ_9 are associated with the level of hygiene awareness among maternal class, vaccinated individuals and hospitalized individuals.

Details of the parameters used in the model are described in Table 1. The flow map of rotavirus disease is presented in Figure 1.

Table 1: Description of parameters used in the mode

| Parameters | Description |
|--------------------------|--|
| $\xi\Omega$ | Inclusion rate into maternal class |
| $\Omega(1 - \rho - \xi)$ | Inclusion rate into susceptible class S_0 |
| $\Omega\rho$ | Inclusion rate into vaccination class V_0 |
| κ | Susceptible rate of maternal class |
| ϕ | Vaccination rate of maternal class |
| α | Vaccination rate of susceptible class S_0 |
| α_1 | Vaccination rate of susceptible class S_1 |
| α_2 | Vaccination rate of susceptible class S_2 |
| Λ | Force of rotavirus infection |
| η | Lower infection risk via maternal antibodies |
| γ | Lower infection risk via vaccination |
| σ | Hospitalization rate of first infection |
| τ | Recovery rate of first infection |
| ψ | Waning rate of temporary immunity |
| σ_1 | Hospitalization rate of second infection |
| τ_1 | Recovery rate of second infection |
| σ_2 | Hospitalization rate of third infection |
| τ_2 | Recovery rate of third infection |
| μ | Natural death rate |
| δ | Rotavirus disease induced rate |

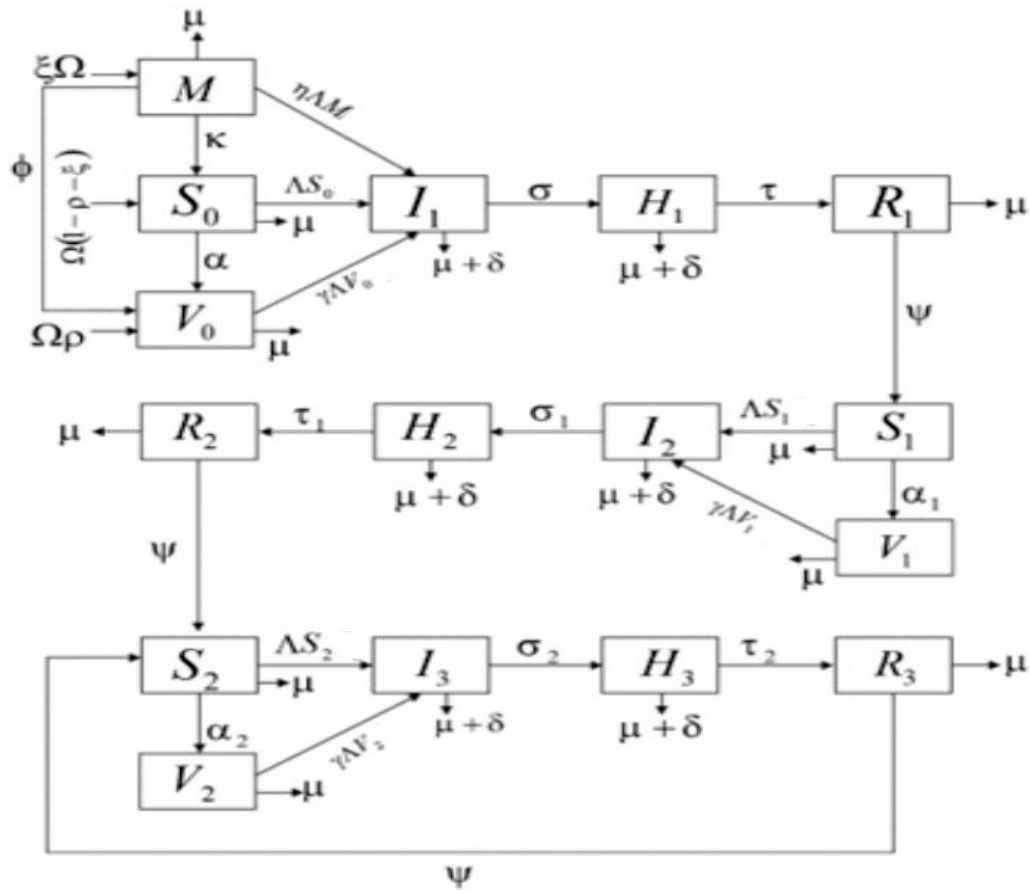


Figure 1: Schematic diagram interaction of each compartment

The equations of the model

$$\left. \begin{aligned}
 M' &= \xi\Omega - \eta\Lambda M - (\phi + \kappa + \mu)M \\
 S_0' &= \Omega(1 - \rho - \xi) + \kappa M - \Lambda S_0 - (\alpha + \mu)S_0 \\
 V_0' &= \rho\Omega + \phi M + \alpha S_0 - \gamma\Lambda V_0 - \mu V_0 \\
 I_1' &= \eta\Lambda M + \Lambda S_0 + \gamma\Lambda V_0 - (\sigma + \mu + \delta)I_1 \\
 H_1' &= \sigma I_1 - (\tau + \mu + \delta)H_1 \\
 R_1' &= \tau H_1 - (\psi + \mu)R_1 \\
 S_1' &= \psi R_1 - \Lambda S_1 - (\alpha_1 + \mu)S_1 \\
 V_1' &= \alpha_1 S_1 - \gamma\Lambda V_1 - \mu V_1 \\
 I_2' &= \Lambda S_1 + \gamma\Lambda V_1 - (\sigma_1 + \mu + \delta)I_2 \\
 H_2' &= \sigma_1 I_2 - (\tau_1 + \mu + \delta)H_2 \\
 R_2' &= \tau_1 H_2 - (\psi + \mu)R_2 \\
 S_2' &= \psi(R_2 + R_3) - \Lambda S_2 - (\alpha_2 + \mu)S_2 \\
 V_2' &= \alpha_2 S_2 - \gamma\Lambda V_2 - \mu V_2 \\
 I_3' &= \Lambda S_2 + \gamma\Lambda V_2 - (\sigma_2 + \mu + \delta)I_3 \\
 H_3' &= \sigma_2 I_3 - (\tau_2 + \mu + \delta)H_3 \\
 R_3' &= \tau_2 H_3 - (\psi + \mu)R_3
 \end{aligned} \right\} \tag{2}$$

with initial condition

$$\begin{aligned}
 M(0) \geq 0, S_0(0) \geq 0, V_0(0) \geq 0, I_1(0) \geq 0, H_1(0) \geq 0, R_1(0) \geq 0 \\
 S_1(0) \geq 0, V_1(0) \geq 0, I_2(0) \geq 0, H_2(0) \geq 0, R_2(0) \geq 0, \\
 S_2(0) \geq 0, V_2(0) \geq 0, I_3(0) \geq 0, H_3(0) \geq 0, R_3(0) \geq 0.
 \end{aligned}$$

Mathematical Analysis of the Rotavirus Model

Non-negativity and boundedness of Solution

The differential equation for the population is as follows:

$$N' = M' + S_0' + V_0' + I_1' + H_1' + R_1' + S_1' + V_1' + I_2' + H_2' + R_2' + S_2' + V_3' + I_3' + H_3' + R_3' \tag{3}$$

Putting equation (2) into equation (3) eliminating correctly, we have

$$\frac{dN}{dt} = \Omega - \mu N + \delta(I_1 + H_1 + I_2 + H_2 + I_3 + H_3) \tag{4}$$

Theorem I: If $(M, S_0, V_0, I_1, H_1, R_1, S_1, V_1, I_2, H_2, R_2, S_2, V_3, I_3, H_3, R_3)$ is the solution of equation (2) with the initial conditions in a biologically feasible region Δ with:

$$\Delta = (M, S_0, V_0, I_1, H_1, R_1, S_1, V_1, I_2, H_2, R_2, S_2, V_3, I_3, H_3, R_3) \in R_+^{16} : N_h \leq \frac{\Omega}{\mu}$$

Then Δ is non-negative invariant.

So, at DFE $\delta = 0$, equation (4) becomes

$$\frac{dN}{dt} = \Omega - \mu N \tag{5}$$

Using integrating factor method, we have'

$$\therefore \lim_{t \rightarrow \infty} N(t) \leq \frac{\Omega}{\mu} \tag{6}$$

Here, we verified the non-negativity of the solution which ensures that the rotavirus model's predictions are physically and epidemiologically plausible, and that it does not generate unrealistic scenarios where the number

of individuals in a particular compartment becomes negative and also the boundedness of the solution was verified, which shows the rotavirus model do not grow unbounded, but rather, their values remain within a defined range or limit. In the rotavirus transmission, the number of individuals in each compartment does not grow indefinitely but remains within realistic bounds. And also the boundedness ensures that the model's predictions do not lead to unrealistic scenarios where the disease spreads uncontrollably and reaches unattainable levels.

Rotavirus-free steady-state.

It need be mentioned that even in the absence disease every individual in the population is vulnerable (i.e., Susceptible). So, then, $S_0^0 \neq 0$, and all other compartments are equal to zero

Thus, the rotavirus model's system of equations (2) gives,

$$\Omega - \mu S_0^0 = 0$$

And this gives

$$S_0^0 = \frac{\Omega}{\mu} \tag{7}$$

We have the Rotavirus-free steady-state for the individuals

$$\left(M, S_0, V_0, I_1, H_1, R_1, S_1, V_1, I_2, H_2, R_2, S_2, V_3, I_3, H_3, R_3 \right) \text{ as,} \tag{8}$$

$$E^0 = \left(0, \frac{\Omega}{\mu}, 0, 0, 0, 0, 0, 0, 0, 0, 0, 0, 0, 0, 0, 0 \right)$$

Basic reproductive ratio

The basic reproductive ration of Rotavirus model's system equation (1) is obtained via the method of next generation matrix formulated by Diekmann and Heesterbeek. Using $R_n = \rho(FV^{-1})$ the new infection terms, F and transition terms, V of system (1) are respectively given as;

$$F = \begin{bmatrix} \eta\Lambda M + \Lambda S_0 + \gamma\Lambda V_0 \\ -\eta\Lambda M \\ -\gamma\Lambda V_0 \\ 0 \\ -\gamma\Lambda V_1 \\ \Lambda S_1 + \gamma\Lambda V_1 \\ 0 \\ -\gamma\Lambda V_2 \\ \Lambda S_2 + \gamma\Lambda V_2 \\ 0 \end{bmatrix} \text{ and, } V = \begin{bmatrix} (\sigma + \mu + \delta)I_1 \\ -\xi\Omega + (\phi + \kappa + \mu)M \\ -\rho\Omega - \phi M - \alpha S_0 + \mu V_0 \\ -\sigma I_1 + (\tau + \mu + \delta)H_1 \\ -\alpha_1 S_1 + \mu V_1 \\ (\sigma_1 + \mu + \delta)I_2 \\ -\sigma_1 I_2 + (\tau_1 + \mu + \delta)H_2 \\ -\alpha_2 S_2 + \mu V_2 \\ (\sigma_2 + \mu + \delta)I_3 \\ -\sigma_2 I_3 + (\tau_2 + \mu + \delta)H_3 \end{bmatrix} \tag{9}$$

Where $\Lambda = \Phi(I_1 + \theta_1 M + \theta_2 V_0 + \theta_3 H_1 + \theta_4 V_1 + \theta_5 I_2 + \theta_6 H_2 + \theta_7 V_2 + \theta_8 I_3 + \theta_9 H_3)$

At E^0 , taking the partial derivatives of F and V gives,

$$\begin{aligned}
 F &= \begin{bmatrix} \frac{\Phi\Omega}{\mu} & \frac{\theta_1\Phi\Omega}{\mu} & \frac{\theta_2\Phi\Omega}{\mu} & \frac{\theta_3\Phi\Omega}{\mu} & \frac{\theta_4\Phi\Omega}{\mu} & \frac{\theta_5\Phi\Omega}{\mu} & \frac{\theta_6\Phi\Omega}{\mu} & \frac{\theta_7\Phi\Omega}{\mu} & \frac{\theta_8\Phi\Omega}{\mu} & \frac{\theta_9\Phi\Omega}{\mu} \\ 0 & 0 & 0 & 0 & 0 & 0 & 0 & 0 & 0 & 0 \\ 0 & 0 & 0 & 0 & 0 & 0 & 0 & 0 & 0 & 0 \\ 0 & 0 & 0 & 0 & 0 & 0 & 0 & 0 & 0 & 0 \\ 0 & 0 & 0 & 0 & 0 & 0 & 0 & 0 & 0 & 0 \\ 0 & 0 & 0 & 0 & 0 & 0 & 0 & 0 & 0 & 0 \\ 0 & 0 & 0 & 0 & 0 & 0 & 0 & 0 & 0 & 0 \\ 0 & 0 & 0 & 0 & 0 & 0 & 0 & 0 & 0 & 0 \\ 0 & 0 & 0 & 0 & 0 & 0 & 0 & 0 & 0 & 0 \\ 0 & 0 & 0 & 0 & 0 & 0 & 0 & 0 & 0 & 0 \end{bmatrix} \\
 V &= \begin{bmatrix} v1 & 0 & 0 & 0 & 0 & 0 & 0 & 0 & 0 & 0 \\ 0 & v2 & 0 & 0 & 0 & 0 & 0 & 0 & 0 & 0 \\ 0 & -\phi & \mu & 0 & 0 & 0 & 0 & 0 & 0 & 0 \\ -\sigma & 0 & 0 & v3 & 0 & 0 & 0 & 0 & 0 & 0 \\ 0 & 0 & 0 & 0 & \mu & 0 & 0 & 0 & 0 & 0 \\ 0 & 0 & 0 & 0 & 0 & v4 & 0 & 0 & 0 & 0 \\ 0 & 0 & 0 & 0 & 0 & -\sigma_1 & v5 & 0 & 0 & 0 \\ 0 & 0 & 0 & 0 & 0 & 0 & 0 & \mu & 0 & 0 \\ 0 & 0 & 0 & 0 & 0 & 0 & 0 & 0 & v6 & 0 \\ 0 & 0 & 0 & 0 & 0 & 0 & 0 & 0 & -\sigma_2 & v7 \end{bmatrix}
 \end{aligned} \tag{10}$$

where $v1 = (\sigma + \mu + \delta)$, $v2 = (\phi + \kappa + \mu)$, $v3 = (\tau + \mu + \delta)$, $v4 = (\sigma_1 + \mu + \delta)$, $v5 = (\tau_1 + \mu + \delta)$, $v6 = (\sigma_2 + \mu + \delta)$ and $v7 = (\tau_2 + \mu + \delta)$

The basic reproductive ration is the same as the spectral radius of the next generation matrix FV^{-1} . Due to the complexity of the model, we make us of Maple 13 to compute the basic reproductive ration and thus, from above, we obtain the expression for R_n as

$$R_n = \rho(FV^{-1}) = \frac{\Phi\Omega}{\mu(\sigma + \mu + \delta)} \left(1 + \frac{\sigma\theta_3}{(\tau + \mu + \delta)} \right) \tag{11}$$

Stability of DFE Point

Theorem II: The disease-free equilibrium of the rotavirus model system (1) is considered locally asymptotically stable (LAS) if all Jacobian eigenvalues of the system have negative real values.

Proof:

To demonstrate the theorem mentioned above, we calculate the Jacobian matrix of the model's system at

$$E^0 = \left(0, \frac{\Omega}{\mu}, 0, 0, 0, 0, 0, 0, 0, 0, 0, 0, 0, 0, 0 \right)$$

The Jacobian matrix, denoted by

$J(M, S_0, V_0, I_1, H_1, R_1, S_1, V_1, I_2, H_2, R_2, S_2, V_3, I_3, H_3, R_3)$ allows us to calculate and assess the eigenvalues of the system. The Jacobian matrix is given as follows:

$$J = \begin{bmatrix}
 -v1 & 0 & 0 & 0 & 0 & 0 & 0 & 0 & 0 & 0 & 0 & 0 & 0 & 0 & 0 & 0 \\
 \kappa - \frac{\Phi\theta_1\Omega}{\mu} & -v2 & -\frac{\Phi\theta_2\Omega}{\mu} & -\frac{\Phi\theta_3\Omega}{\mu} & -\frac{\Phi\theta_4\Omega}{\mu} & 0 & 0 & -\frac{\Phi\theta_5\Omega}{\mu} & -\frac{\Phi\theta_6\Omega}{\mu} & -\frac{\Phi\theta_7\Omega}{\mu} & 0 & 0 & -\frac{\Phi\theta_8\Omega}{\mu} & -\frac{\Phi\theta_9\Omega}{\mu} & -\frac{\Phi\theta_{10}\Omega}{\mu} & 0 \\
 \frac{\Phi}{\mu} & 0 & -\frac{\mu}{\mu} & 0 & 0 & 0 & 0 & 0 & 0 & 0 & 0 & 0 & 0 & 0 & 0 & 0 \\
 \frac{\Phi\theta_1\Omega}{\mu} & 0 & \frac{\Phi\theta_2\Omega}{\mu} & -(v3 - \frac{\Phi\Omega}{\mu}) & \frac{\Phi\theta_3\Omega}{\mu} & 0 & 0 & \frac{\Phi\theta_4\Omega}{\mu} & \frac{\Phi\theta_5\Omega}{\mu} & \frac{\Phi\theta_6\Omega}{\mu} & 0 & 0 & \frac{\Phi\theta_7\Omega}{\mu} & \frac{\Phi\theta_8\Omega}{\mu} & \frac{\Phi\theta_9\Omega}{\mu} & 0 \\
 0 & 0 & 0 & \sigma & -v4 & 0 & 0 & 0 & 0 & 0 & 0 & 0 & 0 & 0 & 0 & 0 \\
 0 & 0 & 0 & 0 & \tau & -v5 & 0 & 0 & 0 & 0 & 0 & 0 & 0 & 0 & 0 & 0 \\
 0 & 0 & 0 & 0 & 0 & \psi & -v6 & 0 & 0 & 0 & 0 & 0 & 0 & 0 & 0 & 0 \\
 0 & 0 & 0 & 0 & 0 & 0 & \alpha_1 & -\mu & 0 & 0 & 0 & 0 & 0 & 0 & 0 & 0 \\
 0 & 0 & 0 & 0 & 0 & 0 & 0 & 0 & -v7 & 0 & 0 & 0 & 0 & 0 & 0 & 0 \\
 0 & 0 & 0 & 0 & 0 & 0 & 0 & 0 & \sigma_1 & -v8 & 0 & 0 & 0 & 0 & 0 & 0 \\
 0 & 0 & 0 & 0 & 0 & 0 & 0 & 0 & 0 & \tau_1 & -v5 & 0 & 0 & 0 & 0 & 0 \\
 0 & 0 & 0 & 0 & 0 & 0 & 0 & 0 & 0 & 0 & \psi & -v9 & 0 & 0 & 0 & 0 \\
 0 & 0 & 0 & 0 & 0 & 0 & 0 & 0 & 0 & 0 & 0 & \alpha_2 & -\mu & 0 & 0 & 0 \\
 0 & 0 & 0 & 0 & 0 & 0 & 0 & 0 & 0 & 0 & 0 & 0 & 0 & -v10 & 0 & 0 \\
 0 & 0 & 0 & 0 & 0 & 0 & 0 & 0 & 0 & 0 & 0 & 0 & 0 & 0 & \sigma_2 & -v11 \\
 0 & 0 & 0 & 0 & 0 & 0 & 0 & 0 & 0 & 0 & 0 & 0 & 0 & 0 & \tau_2 & -v5
 \end{bmatrix} \tag{12)$$

Where $v1 = (\phi + \kappa + \mu)$, $v2 = (\alpha + \mu)$, $v3 = (\sigma + \mu + \delta)$, $v4 = (\tau + \mu + \delta)$, $v5 = (\psi + \mu)$, $v6 = (\alpha_1 + \mu)$, $v7 = (\sigma_1 + \mu + \delta)$, $v8 = (\tau_1 + \mu + \delta)$, $v9 = (\alpha_2 + \mu)$, $v10 = (\sigma_2 + \mu + \delta)$, and $v11 = (\tau_2 + \mu + \delta)$

Clearly, the eigenvalues of matrix J are represented by the diagonal elements in the matrix shown above (Idowu et al 2023). It is evident that these eigenvalues are purely real and do not contain any complex components. The signs of these eigenvalues are of utmost importance in determining the stability of the Disease-Free Equilibrium (DFE). In this specific situation, all eigenvalues have negative real components, confirming the local asymptotic stability of the rotavirus at the DFE.

Existence of the endemic equilibrium points

The endemic equilibrium points are defined as

$$E^* = (M^*, S_0^*, V_0^*, I_1^*, H_1^*, R_1^*, S_1^*, V_1^*, I_2^*, H_2^*, R_2^*, S_2^*, V_3^*, I_3^*, H_3^*, R_3^*) \text{ satisfying}$$

$$M' = S_0' = V_0' = I_1' = H_1' = R_1' = S_1' = V_1' = I_2' = H_2' = R_2' = S_2' = V_3' = I_3' = H_3' = R_3' = 0, \tag{13)$$

by equating equation (1) to 0, we have;

$$\left. \begin{aligned}
 0 &= \xi\Omega - \eta\Lambda M^* - (\phi + \kappa + \mu)M^* \\
 0 &= \Omega(1 - \rho - \xi) + \kappa M^* - \Lambda S_0^* - (\alpha + \mu)S_0^* \\
 0 &= \rho\Omega + \phi M^* + \alpha S_0^* - \gamma\Lambda V_0^* - \mu V_0^* \\
 0 &= \eta\Lambda M^* + \Lambda S_0^* + \gamma\Lambda V_0^* - (\sigma + \mu + \delta)I_1^* \\
 0 &= \sigma I_1^* - (\tau + \mu + \delta)H_1^* \\
 0 &= \tau H_1^* - (\psi + \mu)R_1^* \\
 0 &= \psi R_1^* - \Lambda S_1^* - (\alpha_1 + \mu)S_1^* \\
 0 &= \alpha_1 S_1^* - \gamma\Lambda V_1^* - \mu V_1^* \\
 0 &= \Lambda S_1^* + \gamma\Lambda V_1^* - (\sigma_1 + \mu + \delta)I_2^* \\
 0 &= \sigma_1 I_2^* - (\tau_1 + \mu + \delta)H_2^* \\
 0 &= \tau_1 H_2^* - (\psi + \mu)R_2^* \\
 0 &= \psi(R_2^* + R_3^*) - \Lambda S_2^* - (\alpha_2 + \mu)S_2^* \\
 0 &= \alpha_2 S_2^* - \gamma\Lambda V_2^* - \mu V_2^* \\
 0 &= \Lambda S_2^* + \gamma\Lambda V_2^* - (\sigma_2 + \mu + \delta)I_3^* \\
 0 &= \sigma_2 I_3^* - (\tau_2 + \mu + \delta)H_3^* \\
 0 &= \tau_2 H_3^* - (\psi + \mu)R_3^*
 \end{aligned} \right\} \tag{14)$$

Where $\Lambda = \Phi(I_1 + \theta_1 M + \theta_2 V_0 + \theta_3 H_1 + \theta_4 V_1 + \theta_5 I_2 + \theta_6 H_2 + \theta_7 V_2 + \theta_8 I_3 + \theta_9 H_3)$

$$\begin{aligned}
 M^* &= \frac{\xi\Omega}{\eta\Lambda + (\phi + \kappa + \mu)}, \\
 S_0^* &= \frac{\Omega(1 - \rho - \xi) + \kappa\xi\Omega}{(\Lambda + (\alpha + \mu))(\eta\Lambda + (\phi + \kappa + \mu))}, \\
 V_0^* &= \frac{\rho\Omega(\Lambda + (\alpha + \mu))(\eta\Lambda + (\phi + \kappa + \mu)) + \phi\xi\Omega(\Lambda + (\alpha + \mu)) + \alpha(\Omega(1 - \rho - \xi) + \kappa\xi\Omega)}{(\gamma\Lambda + \mu)(\Lambda + (\alpha + \mu))(\eta\Lambda + (\phi + \kappa + \mu))}, \\
 I_1^* &= \frac{\eta\Lambda\xi\Omega(\gamma\Lambda + \mu)(\Lambda + (\alpha + \mu)) + (\gamma\Lambda + \mu)\Lambda(\Omega(1 - \rho - \xi) + \kappa\xi\Omega) + \rho\Omega(\Lambda + (\alpha + \mu))(\eta\Lambda + (\phi + \kappa + \mu)) + \phi\xi\Omega(\Lambda + (\alpha + \mu)) + \alpha(\Omega(1 - \rho - \xi) + \kappa\xi\Omega)}{(\sigma + \mu + \delta)(\gamma\Lambda + \mu)(\Lambda + (\alpha + \mu))(\eta\Lambda + (\phi + \kappa + \mu))}, \\
 H_1^* &= \frac{\sigma}{(\tau + \mu + \delta)} \left[\frac{\eta\Lambda\xi\Omega(\gamma\Lambda + \mu)(\Lambda + (\alpha + \mu)) + (\gamma\Lambda + \mu)\Lambda(\Omega(1 - \rho - \xi) + \kappa\xi\Omega) + \rho\Omega(\Lambda + (\alpha + \mu))(\eta\Lambda + (\phi + \kappa + \mu)) + \phi\xi\Omega(\Lambda + (\alpha + \mu)) + \alpha(\Omega(1 - \rho - \xi) + \kappa\xi\Omega)}{(\sigma + \mu + \delta)(\gamma\Lambda + \mu)(\Lambda + (\alpha + \mu))(\eta\Lambda + (\phi + \kappa + \mu))} \right], \\
 R_1^* &= \frac{\tau\sigma}{(\psi + \mu)(\tau + \mu + \delta)} \left[\frac{\eta\Lambda\xi\Omega(\gamma\Lambda + \mu)(\Lambda + (\alpha + \mu)) + (\gamma\Lambda + \mu)\Lambda(\Omega(1 - \rho - \xi) + \kappa\xi\Omega) + \rho\Omega(\Lambda + (\alpha + \mu))(\eta\Lambda + (\phi + \kappa + \mu)) + \phi\xi\Omega(\Lambda + (\alpha + \mu)) + \alpha(\Omega(1 - \rho - \xi) + \kappa\xi\Omega)}{(\sigma + \mu + \delta)(\gamma\Lambda + \mu)(\Lambda + (\alpha + \mu))(\eta\Lambda + (\phi + \kappa + \mu))} \right], \\
 S_1^* &= \frac{\psi\tau\sigma}{(\Lambda + (\alpha + \mu))(\psi + \mu)(\tau + \mu + \delta)} \left[\frac{\eta\Lambda\xi\Omega(\gamma\Lambda + \mu)(\Lambda + (\alpha + \mu)) + (\gamma\Lambda + \mu)\Lambda(\Omega(1 - \rho - \xi) + \kappa\xi\Omega) + \rho\Omega(\Lambda + (\alpha + \mu))(\eta\Lambda + (\phi + \kappa + \mu)) + \phi\xi\Omega(\Lambda + (\alpha + \mu)) + \alpha(\Omega(1 - \rho - \xi) + \kappa\xi\Omega)}{(\sigma + \mu + \delta)(\gamma\Lambda + \mu)(\Lambda + (\alpha + \mu))(\eta\Lambda + (\phi + \kappa + \mu))} \right], \\
 V_1^* &= \frac{\alpha\psi\tau\sigma}{(\gamma\Lambda V_1^* + \mu)(\Lambda + (\alpha + \mu))(\psi + \mu)(\tau + \mu + \delta)} \left[\frac{\eta\Lambda\xi\Omega(\gamma\Lambda + \mu)(\Lambda + (\alpha + \mu)) + (\gamma\Lambda + \mu)\Lambda(\Omega(1 - \rho - \xi) + \kappa\xi\Omega) + \rho\Omega(\Lambda + (\alpha + \mu))(\eta\Lambda + (\phi + \kappa + \mu)) + \phi\xi\Omega(\Lambda + (\alpha + \mu)) + \alpha(\Omega(1 - \rho - \xi) + \kappa\xi\Omega)}{(\sigma + \mu + \delta)(\gamma\Lambda + \mu)(\Lambda + (\alpha + \mu))(\eta\Lambda + (\phi + \kappa + \mu))} \right], \\
 I_2^* &= \frac{\Lambda S_1^* + \gamma\Lambda V_1^*}{(\sigma_1 + \mu + \delta)}; \quad H_2^* = \frac{\sigma_1(\Lambda S_1^* + \gamma\Lambda V_1^*)}{(\tau_1 + \mu + \delta)(\sigma_1 + \mu + \delta)}; \quad R_2^* = \frac{\tau_1\sigma_1(\Lambda S_1^* + \gamma\Lambda V_1^*)}{(\psi + \mu)(\tau_1 + \mu + \delta)(\sigma_1 + \mu + \delta)}, \\
 S_2^* &= \frac{\psi}{\Lambda + \alpha_2 + \mu} \left(\frac{\tau_1\sigma_1(\Lambda S_1^* + \gamma\Lambda V_1^*)}{(\psi + \mu)(\tau_1 + \mu + \delta)(\sigma_1 + \mu + \delta)} + R_3^* \right), \\
 V_2^* &= \frac{\alpha_2\psi}{(\gamma\Lambda + \mu)(\Lambda + \alpha_2 + \mu)} \left(\frac{\tau_1\sigma_1(\Lambda S_1^* + \gamma\Lambda V_1^*)}{(\psi + \mu)(\tau_1 + \mu + \delta)(\sigma_1 + \mu + \delta)} + R_3^* \right), \\
 I_3^* &= \frac{\left(\frac{\tau_1\sigma_1(\Lambda S_1^* + \gamma\Lambda V_1^*)}{(\psi + \mu)(\tau_1 + \mu + \delta)(\sigma_1 + \mu + \delta)} + R_3^* \right) \left[\frac{\Lambda\psi}{\Lambda + \alpha_2 + \mu} + \frac{\gamma\Lambda\alpha_2\psi}{(\gamma\Lambda + \mu)(\Lambda + \alpha_2 + \mu)} \right]}{(\sigma_2 + \mu + \delta)}, \\
 H_3^* &= \frac{\sigma_2 \left(\frac{\tau_1\sigma_1(\Lambda S_1^* + \gamma\Lambda V_1^*)}{(\psi + \mu)(\tau_1 + \mu + \delta)(\sigma_1 + \mu + \delta)} + R_3^* \right) \left[\frac{\Lambda\psi}{\Lambda + \alpha_2 + \mu} + \frac{\gamma\Lambda\alpha_2\psi}{(\gamma\Lambda + \mu)(\Lambda + \alpha_2 + \mu)} \right]}{(\tau_2 + \mu + \delta)(\sigma_2 + \mu + \delta)}, \\
 R_3^* &= \frac{\tau_2\sigma_2 \left(\frac{\tau_1\sigma_1(\Lambda S_1^* + \gamma\Lambda V_1^*)}{(\psi + \mu)(\tau_1 + \mu + \delta)(\sigma_1 + \mu + \delta)} + R_3^* \right) \left[\frac{\Lambda\psi}{\Lambda + \alpha_2 + \mu} + \frac{\gamma\Lambda\alpha_2\psi}{(\gamma\Lambda + \mu)(\Lambda + \alpha_2 + \mu)} \right]}{(\psi + \mu)(\tau_2 + \mu + \delta)(\sigma_2 + \mu + \delta)}.
 \end{aligned}$$

Utilizing conventional methodologies, the model exhibits disease-free dynamics at equilibrium point E^0 .

Sensitivity analysis of the Rotavirus model

So, we perform an analysis of the reproductive ratiom R_n of the model which checks for the variation and effect of a parameter on R_n when increased or decreased.

Definition: The Normalized Forward-Sensitivity Index of a variable X, which exhibits differential dependency on parameter Y, is outlined as follows:

$$X_Y^X = \frac{\partial X}{\partial Y} \cdot \frac{Y}{X} \tag{15}$$

Concerning the model parameters, we will proceed to calculate the sensitivity indices for the basic reproductive ratio R_n denoted as

$$R_n = \frac{\Phi\Omega}{\mu(\sigma + \mu + \delta)} \left(1 + \frac{\sigma\theta_3}{(\tau + \mu + \delta)} \right).$$

Sensitivity index for Φ

The Normalized Forward-Sensitivity Index of Φ is given by:

$$X_\Phi^{R_n} = \frac{\partial R_n}{\partial \Phi} \cdot \frac{\Phi}{R_n} \tag{16}$$

Calculating and evaluating the derivatives in (16) gives;

$$X_\Phi^{R_n} = \frac{\partial R_n}{\partial \Phi} \cdot \frac{\Phi}{R_n} = \frac{1}{\Phi} R_n \cdot \frac{\Phi}{R_n}$$

$\therefore X_\lambda^{R_n} = +1$ (17)

This yields the sensitivity index λ .

The sensitivity indices of all other parameters in the fundamental reproductive ratio are also obtained using the same procedure, which is consistently applied. Therefore, the sensitivity indices of the parameters are listed below in Table 2, and their visual implications are seen in Figure 2 and Figure 3.

Table 2: Sensitivity indices about additional parameters within the context of the basic reproductive ratio.

| Paramete rs | Values | Source | Index sign | Sensitivity value | Index |
|-------------|---------|-----------------------|------------|-------------------|-------|
| Φ | 0.5 | Ali Raza et-al (2022) | + | 1 | |
| Ω | 0.5 | Ali Raza et-al (2022) | + | 1 | |
| θ_3 | 0.35 | SCIENCE DIRECT | + | 0.01190476 | |
| σ | 0.2-0.9 | ASSUME | - | -0.1050543 | |
| μ | 0.01 | Ali Raza et-al (2022) | - | -1.0058684 | |
| δ | 1.5 | Ali Raza et-al (2022) | - | -0.8802665 | |
| τ | 4.3 | NIHMS | - | -0.0088108 | |

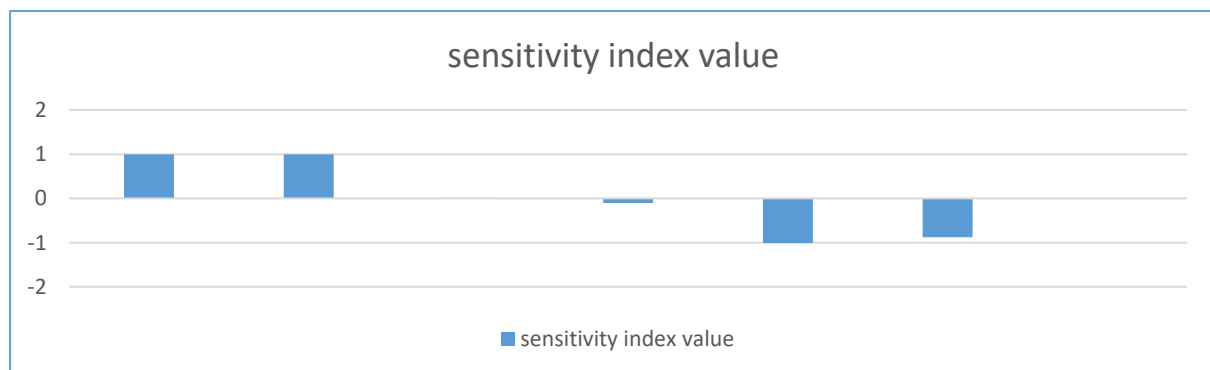


Figure 2: Visual depiction of parameter sensitivity

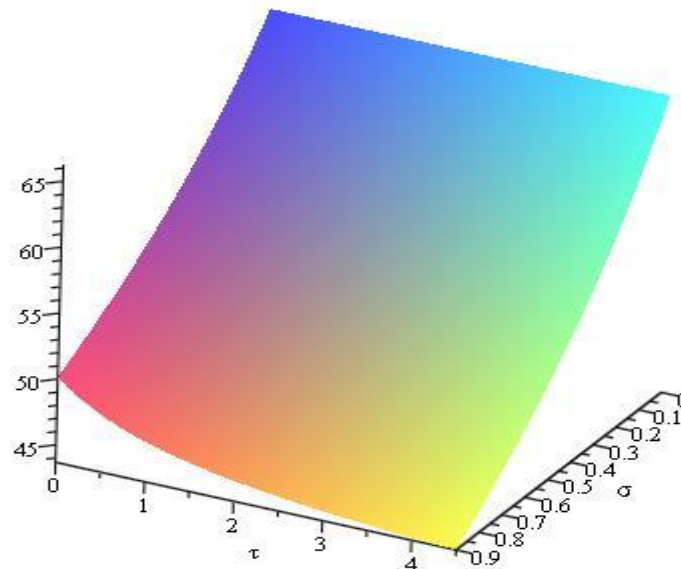


Figure 3: Effect of ω_1 and ω_2 on R_n

Optimal Control Strategies for Rotavirus

Here are some key components of optimal control for rotavirus: For first infection, C_1 connotes prenatal education about the importance of vaccination and vaccination during pregnancy. C_2 connotes routine vaccination of infants and young children with rotavirus vaccines. C_3 connotes isolation and medical care of infected individuals. C_4 connotes implementation of infection control measures and supportive care to hospitalized patients and, C_5 connotes immunity monitoring and booster vaccination for individuals who have recovered. For the second infection, C_6 connotes the effort to ensure that children receive the recommended doses of rotavirus vaccines including booster shots. C_7 connotes the continuation of isolated and medical care of infected individuals. C_8 connotes continuation of implementation of infection control measures and supportive care to hospitalized patients, and C_9 connotes continuation of immunity monitoring and booster vaccination for individuals who have recovered. For the third infection, it C_{10} connotes the effort to ensure that children receive the recommended doses of rotavirus vaccines, including booster shots to maintain immunity against repeated infections. C_{11} Connotes the continuation of isolated and medical care to manage symptoms, reduce virus shedding, and prevent complications. Maintaining strict infection control measures in healthcare settings involves continuously monitoring recovered individuals for immunity levels and frequent booster vaccinations for individuals. Based on these assumptions, the following set of new equations is derived:

$$\left. \begin{aligned}
M' &= \xi\Omega - (1 - C_1)\eta\Lambda M - (C_1 + \kappa + \mu)M \\
S_0' &= \Omega(1 - \rho - \xi) + \kappa M - (1 - C_2)\Lambda S_0 - (C_2 + \mu)S_0 \\
V_0' &= \rho\Omega + C_1 M + C_2 S_0 - (1 - C_3)\gamma\Lambda V_0 - \mu V_0 \\
I_1' &= (1 - C_1)\eta\Lambda M + (1 - C_2)\Lambda S_0 + (1 - C_3)\gamma\Lambda V_0 - (C_4 + \mu + \delta)I_1 \\
H_1' &= C_4 I_1 - (\tau + \mu + \delta)H_1 \\
R_1' &= \tau H_1 - ((1 - C_5)\psi + \mu)R_1 \\
S_1' &= (1 - C_5)\psi R_1 - (1 - C_6)\Lambda S_1 - (C_6 + \mu)S_1 \\
V_1' &= C_6 S_1 - (1 - C_7)\gamma\Lambda V_1 - \mu V_1 \\
I_2' &= (1 - C_6)\Lambda S_1 + (1 - C_7)\gamma\Lambda V_1 - (C_8 + \mu + \delta)I_2 \\
H_2' &= C_8 I_2 - (\tau_1 + \mu + \delta)H_2 \\
R_2' &= \tau_1 H_2 - ((1 - C_9)\psi + \mu)R_2 \\
S_2' &= (1 - C_9)\psi R_2 + (1 - C_{13})\psi R_3 - (1 - C_{10})\Lambda S_2 - (C_{10} + \mu)S_2 \\
V_2' &= C_{10} S_2 - (1 - C_{11})\gamma\Lambda V_2 - \mu V_2 \\
I_3' &= (1 - C_{10})\Lambda S_2 + (1 - C_{11})\gamma\Lambda V_2 - (C_{12} + \mu + \delta)I_3 \\
H_3' &= C_{12} I_3 - (\tau_2 + \mu + \delta)H_3 \\
R_3' &= \tau_2 H_3 - ((1 - C_{13})\psi + \mu)R_3
\end{aligned} \right\} \quad (18)$$

Analysis of the Model Incorporating Preventive Measures

Within this segment, we constructed a model centered on an objective functional framework, showcasing the potential for manipulation through the utilization of Pontryagin's Maximum Principle. By focusing on the optimal configuration outlined in the system of equations (18), we have highlighted the emergence of a significant control concern, which we subsequently elucidated before delving into its comprehensive global optimization. The intricate task of selecting the most efficacious strategies is encapsulated by the objective functional denoted as H . The overarching pre-established aim entails the minimization of the populace in all classes, all within a designated time interval $[0, K]$.

Let $L = \{(C_1, C_2, C_3, C_4, C_5, C_6, C_7, C_8, C_9, C_{10}, C_{11}, C_{12}, C_{13}) \in L\}$ be Lebesgue measurable on $[0, 1]$,

Where $0 \leq C_i(t) \leq 1 \in [0, 1], i = 1, 2, 3, 4, 5, 6, 7, 8, 9, 10, 11, 12, 13$

Then, we have the objective function, O , to be

$$O(C) = \int_0^K (T_1 R_3 + T_2 H_3 + T_3 V_2 + T_4 S_2 + T_5 R_2 + T_6 H_2 + T_7 V_1 + T_8 S_1 + T_9 R_1 + T_{10} H_1 + T_{11} V_0 + T_{12} S_0 + T_{13} M + \frac{1}{2}(U)) dt \quad (19)$$

Where, $C = C_1, C_2, C_3, C_4, C_5, C_6, C_7, C_8, C_9, C_{10}, C_{11}, C_{12}, C_{13}$

$$\text{and } U = U_1 C_1^2 + U_2 C_2^2 + U_3 C_3^2 + U_4 C_4^2 + U_5 C_5^2 + U_6 C_6^2 + U_7 C_7^2 + U_8 C_8^2 + U_9 C_9^2 \\
+ U_{10} C_{10}^2 + U_{11} C_{11}^2 + U_{12} C_{12}^2 + U_{13} C_{13}^2$$

constraint to (18)

The terminal time point is represented by the value K , while the coefficients T_1 to T_{13} correspond to the weight constants attributed to the virus within distinct groups. The primary objective of this section centers on the reduction of the operational expenditure as indicated by equation (19). Furthermore, our investigation extends to encompass an analysis of the social cost $U_{13} C_{13}^2$ associated with the described scenario.

In order to fulfil the aim of addressing the control problem, we endeavour to identify the functions;

$$\left(C_1^*(t), C_2^*(t), C_3^*(t), C_4^*(t), C_5^*(t), C_6^*(t), C_7^*(t), C_8^*(t), C_9^*(t), C_{10}^*(t), C_{11}^*(t), C_{12}^*(t), C_{13}^*(t) \right), \text{ such that } \mathcal{O}(C^*) = \min \{ \mathcal{O}(C), (C) \in L \} \tag{20}$$

Where, $C^* = C_1^*(t), C_2^*(t), C_3^*(t), C_4^*(t), C_5^*(t), C_6^*(t), C_7^*(t), C_8^*(t), C_9^*(t), C_{10}^*(t), C_{11}^*(t), C_{12}^*(t), C_{13}^*(t)$

Existence of an Optimal Control Solution

Theorem: From equation (20), Consider $\mathcal{O}(C)$, subject to (18) and with $t=0$ be the initial condition, then given the optimal control to be C^* such that

$$\mathcal{O}(C^*) = \min \{ \mathcal{O}(C), (C) \in L \}$$

Proof: Because the integrand of \mathcal{O} demonstrates convexity concerning the control measures C the existence of an optimal control solution is ensured.

Next, it is essential to demonstrate the optimal solution. The Lagrangian is expressed as follows:

$$G = T_1 R_3 + T_2 H_3 + T_3 V_2 + T_4 S_2 + T_5 R_2 + T_6 H_2 + T_7 V_1 + T_8 S_1 + T_9 R_1 + T_{10} H_1 + T_{11} V_0 + T_{12} S_0 + T_{13} M + \frac{1}{2}(U)t \tag{21}$$

where
$$U = U_1 C_1^2 + U_2 C_2^2 + U_3 C_3^2 + U_4 C_4^2 + U_5 C_5^2 + U_6 C_6^2 + U_7 C_7^2 + U_8 C_8^2 + U_9 C_9^2 + U_{10} C_{10}^2 + U_{11} C_{11}^2 + U_{12} C_{12}^2 + U_{13} C_{13}^2$$

The Hamiltonian function is given as;

$$\begin{aligned} H = & T_1 R_3 + T_2 H_3 + T_3 V_2 + T_4 S_2 + T_5 R_2 + T_6 H_2 + T_7 V_1 + T_8 S_1 + T_9 R_1 + T_{10} H_1 + T_{11} V_0 + T_{12} S_0 + T_{13} M + \frac{1}{2}(U)t \\ & + \Psi_M [M'] + \Psi_{S_0} [S_0'] + \Psi_{V_0} [V_0'] + \Psi_{I_1} [I_1'] + \Psi_{H_1} [H_1'] + \Psi_{R_1} [R_1'] \\ & + \Psi_{S_1} [S_1'] + \Psi_{V_1} [V_1'] + \Psi_{I_2} [I_2'] + \Psi_{H_2} [H_2'] + \Psi_{R_2} [R_2'] \\ & + \Psi_{S_2} [S_2'] + \Psi_{V_2} [V_2'] + \Psi_{I_3} [I_3'] + \Psi_{H_3} [H_3'] + \Psi_{R_3} [R_3'] \end{aligned} \tag{22}$$

Given are distinct and non-overlapping variables.

We are now poised to employ the essential conditions to the Hamiltonian for analysis.

To unveil the adjoint equation and fulfill the transversality condition, we leverage the Hamiltonian H . Through the process of differentiation, we ascertain the values concerning the variables with respect to the Hamiltonian.

This leads us to the formulation of the adjoint equation, which is expressed as follows:

$$\frac{d\Psi_M}{dt} = -\frac{\partial H}{dM} = \left[\begin{aligned} & -T_{13} + ((1-C_1)\eta(\Phi\theta_1 M + \Lambda) - (C_1 + \kappa + \mu))\Psi_M \\ & + (-\kappa + (1-C_2)\Phi\theta_1 S_0)\Psi_{S_0} + (-C_1 + (1-C_3)\gamma\Phi\theta_1 V_0)\Psi_{V_0} - \left(\frac{(1-C_1)\eta(\Phi\theta_1 M + \Lambda)}{(1-C_2)\Phi\theta_1 S_0 + (1-C_3)\gamma\Phi\theta_1 V_0} \right) \Psi_{I_1} \end{aligned} \right] \tag{23}$$

$$\frac{d\Psi_{S_0}}{dt} = -\frac{\partial H}{dS_0} = \left[-T_{12} + ((1-C_2)\Lambda + (C_2 + \mu))\Psi_{S_0} - C_2\Psi_{V_0} - ((1-C_2)\Lambda)\Psi_{I_1} \right] \tag{24}$$

$$\frac{d\Psi_{V_0}}{dt} = -\frac{\partial H}{dV_0} = \left[\begin{aligned} & -T_{11} + (1-C_1)\eta\Phi\theta_2 M\Psi_M + (1-C_2)\Phi\theta_2 S_0\Psi_{S_0} + ((1-C_3)\gamma(\Phi\theta_2 V_0 + \Lambda) + \mu)\Psi_{V_0} \\ & - \left(\frac{(1-C_1)\eta\Phi\theta_2 M + (1-C_2)\Phi\theta_2 S_0}{(1-C_3)\gamma(\Phi\theta_2 V_0 + \Lambda)} \right) \Psi_{I_1} + ((1-C_6)\Phi\theta_2 S_1)\Psi_{S_1} + (1-C_7)\gamma\Phi\theta_2 V_1\Psi_{V_1} \\ & - ((1-C_6)\Phi\theta_2 S_1 + (1-C_7)\gamma\Phi\theta_2 V_1)\Psi_{I_2} + ((1-C_{10})\Phi\theta_2 S_2)\Psi_{S_2} \\ & + (1-C_{11})\gamma\Phi\theta_2 V_2\Psi_{V_2} - ((1-C_{10})\Phi\theta_2 S_2 + (1-C_{11})\gamma\Phi\theta_2 V_2)\Psi_{I_3} \end{aligned} \right] \tag{25}$$

$$\frac{d\Psi_{I_1}}{dt} = -\frac{\partial H}{\partial I_1} = \left[\begin{aligned} & (1-C_1)\eta\Phi M\Psi_M + (1-C_2)\Phi S_0\Psi_{S_0} + (1-C_3)\gamma\Phi V_0\Psi_{V_0} \\ & - \left((1-C_1)\eta\Phi M + (1-C_2)\Phi S_0 \right. \\ & \quad \left. + (1-C_3)\gamma\Phi V_0 + (C_4 + \mu + \delta) \right) \Psi_{I_1} - C_4\Psi_{H_1} \\ & + (1-C_6)\Phi S_1\Psi_{S_1} + (1-C_7)\gamma\Phi V_1\Psi_{V_1} - ((1-C_6)\Phi S_1 + (1-C_7)\gamma\Phi V_1)\Psi_{I_2} \\ & + ((1-C_{10})S_2)\Phi\Psi_{S_2} + (1-C_{11})\gamma\Phi V_2\Psi_{V_2} - ((1-C_{10})\Phi S_2 + (1-C_{11})\gamma\Phi V_2)\Psi_{I_3} \end{aligned} \right] \quad (26)$$

$$\frac{d\Psi_{H_1}}{dt} = -\frac{\partial H}{\partial H_1} = \left[\begin{aligned} & -T_{10} + (1-C_1)\eta\Phi\theta_3 M\Psi_M + (1-C_2)\Phi\theta_3 S_0\Psi_{S_0} + (1-C_3)\gamma\Phi\theta_3 V_0\Psi_{V_0} \\ & - \left((1-C_1)\eta\Phi\theta_3 M + (1-C_2)\Phi\theta_3 S_0 \right. \\ & \quad \left. + (1-C_3)\gamma\Phi\theta_3 V_0 \right) \Psi_{I_1} + (\tau + \mu + \delta)\Psi_{H_1} - \tau\Psi_{R_1} \\ & + ((1-C_6)\Phi\theta_3 S_1)\Psi_{S_1} + (1-C_7)\gamma\Phi\theta_3 V_1\Psi_{V_1} \\ & - ((1-C_6)\Phi\theta_3 S_1 + (1-C_7)\gamma\Phi\theta_3 V_1)\Psi_{I_2} + ((1-C_{10})\Phi\theta_3 S_2)\Psi_{S_2} \\ & + (1-C_{11})\gamma\Phi\theta_3 V_2\Psi_{V_2} - ((1-C_{10})\Phi\theta_3 S_2 + (1-C_{11})\gamma\Phi\theta_3 V_2)\Psi_{I_3} \end{aligned} \right] \quad (27)$$

$$\frac{d\Psi_{R_1}}{dt} = -\frac{\partial H}{\partial R_1} = \left[-T_9 + ((1-C_5)\nu + \mu)\Psi_{R_1} - (1-C_5)\nu\Psi_{S_1} \right] \quad (28)$$

$$\frac{d\Psi_{S_1}}{dt} = -\frac{\partial H}{\partial S_1} = \left[-T_8 + ((1-C_6)\Lambda + (C_6 + \mu))\Psi_{S_1} - C_6\Psi_{V_1} - (1-C_6)\Lambda\Psi_{I_2} \right] \quad (29)$$

$$\frac{d\Psi_{V_1}}{dt} = -\frac{\partial H}{\partial V_1} = \left[\begin{aligned} & -T_7 + (1-C_1)\eta\Phi\theta_4 M\Psi_M + (1-C_2)\Phi\theta_4 S_0\Psi_{S_0} + ((1-C_3)\gamma\Phi\theta_4 V_0)\Psi_{V_0} \\ & - \left((1-C_1)\eta\Phi\theta_4 M + (1-C_2)\Phi\theta_4 S_0 \right. \\ & \quad \left. + (1-C_3)\gamma\Phi\theta_4 V_0 \right) \Psi_{I_1} + ((1-C_6)\Phi\theta_4 S_1)\Psi_{S_1} + ((1-C_7)\gamma(\Phi\theta_4 V_1 + \Lambda) + \mu)\Psi_{V_1} \\ & - ((1-C_6)\Phi\theta_4 S_1 + (1-C_7)\gamma(\Phi\theta_4 V_1 + \Lambda))\Psi_{I_2} + ((1-C_{10})\Phi\theta_4 S_2)\Psi_{S_2} \\ & + (1-C_{11})\gamma\Phi\theta_4 V_2\Psi_{V_2} - ((1-C_{10})\Phi\theta_4 S_2 + (1-C_{11})\gamma\Phi\theta_4 V_2)\Psi_{I_3} \end{aligned} \right] \quad (30)$$

$$\frac{d\Psi_{I_2}}{dt} = -\frac{\partial H}{\partial I_2} = \left[\begin{aligned} & (1-C_1)\eta\Phi\theta_5 M\Psi_M + (1-C_2)\Phi\theta_5 S_0\Psi_{S_0} + (1-C_3)\gamma\Phi\theta_5 V_0\Psi_{V_0} \\ & - \left((1-C_1)\eta\Phi\theta_5 M + (1-C_2)\Phi\theta_5 S_0 \right. \\ & \quad \left. + (1-C_3)\gamma\Phi\theta_5 V_0 \right) \Psi_{I_1} + (1-C_6)\Phi\theta_5 S_1\Psi_{S_1} + (1-C_7)\gamma\Phi\theta_5 V_1\Psi_{V_1} \\ & - ((1-C_6)\Phi\theta_5 S_1 + (1-C_7)\gamma\Phi\theta_5 V_1 - (C_8 + \mu + \delta))\Psi_{I_2} - C_8\Psi_{H_2} \\ & + ((1-C_{10})\Phi\theta_5 S_2)\Psi_{S_2} + (1-C_{11})\gamma\Phi\theta_5 V_2\Psi_{V_2} - ((1-C_{10})\Phi\theta_5 S_2 + (1-C_{11})\gamma\Phi\theta_5 V_2)\Psi_{I_3} \end{aligned} \right] \quad (31)$$

$$\frac{d\Psi_{H_2}}{dt} = -\frac{\partial H}{\partial H_2} = \left[\begin{aligned} & -T_6 + (1-C_1)\eta\Phi\theta_6 M\Psi_M + (1-C_2)\Phi\theta_6 S_0\Psi_{S_0} + (1-C_3)\gamma\Phi\theta_6 V_0\Psi_{V_0} \\ & - \left((1-C_1)\eta\Phi\theta_6 M + (1-C_2)\Phi\theta_6 S_0 \right. \\ & \quad \left. + (1-C_3)\gamma\Phi\theta_6 V_0 \right) \Psi_{I_1} + (1-C_6)\Phi\theta_6 S_1\Psi_{S_1} + (1-C_7)\gamma\Phi\theta_6 V_1\Psi_{V_1} \\ & - ((1-C_6)\Phi\theta_6 S_1 + (1-C_7)\gamma\Phi\theta_6 V_1)\Psi_{I_2} + (\tau_1 + \mu + \delta)\Psi_{H_2} - \tau_1\Psi_{R_2} \\ & + (1-C_{10})\Phi\theta_6 S_2\Psi_{S_2} + (1-C_{11})\gamma\Phi\theta_6 V_2\Psi_{V_2} - ((1-C_{10})\Phi\theta_6 S_2 + (1-C_{11})\gamma\Phi\theta_6 V_2)\Psi_{I_3} \end{aligned} \right] \quad (32)$$

$$\frac{d\Psi_{R_2}}{dt} = -\frac{\partial H}{\partial R_2} = \left[-T_5 + ((1-C_9)\nu + \mu)\Psi_{R_2} - (1-C_9)\nu\Psi_{S_2} \right] \quad (33)$$

$$\frac{d\Psi_{S_2}}{dt} = -\frac{\partial H}{\partial S_2} = \left[-T_4 + ((1-C_{10})\Lambda + (C_{10} + \mu))\Psi_{S_0} - C_{10}\Psi_{V_2} - ((1-C_{10})\Lambda)\Psi_{I_3} \right] \quad (34)$$

$$\frac{d\Psi_{V_2}}{dt} = -\frac{\partial H}{dV_2} = \left[\begin{array}{l} -T_3 + (1-C_1)\eta\Phi\theta_7M\Psi_M + (1-C_2)\Phi\theta_7S_0\Psi_{S_0} + (1-C_3)\gamma\Phi\theta_7V_0\Psi_{V_0} \\ -\left(\frac{(1-C_1)\eta\Phi\theta_7M + (1-C_2)\Phi\theta_7S_0}{(1-C_3)\gamma\Phi\theta_7V_0} \right) \Psi_{I_1} + (1-C_6)\Phi\theta_7S_1\Psi_{S_1} + (1-C_7)\gamma\Phi\theta_7V_1\Psi_{V_1} \\ -((1-C_6)\Phi\theta_7S_1 + (1-C_7)\gamma\Phi\theta_7V_1)\Psi_{I_2} + (1-C_{10})\Phi\theta_7S_2\Psi_{S_2} + ((1-C_{11})\gamma(\Phi\theta_7V_2 + \Lambda) + \mu)\Psi_{V_2} \\ -((1-C_{10})\Phi\theta_7S_2 + (1-C_{11})\gamma(\Phi\theta_7V_2 + \Lambda))\Psi_{I_3} \end{array} \right] \quad (35)$$

$$\frac{d\Psi_{H_3}}{dt} = -\frac{\partial H}{dH_3} = \left[\begin{array}{l} -T_2 + (1-C_1)\eta\Phi\theta_9M\Psi_M + (1-C_2)\Phi\theta_9S_0\Psi_{S_0} + (1-C_3)\gamma\Phi\theta_9V_0\Psi_{V_0} - \left(\frac{(1-C_1)\eta\Phi\theta_9M + (1-C_2)\Phi\theta_9S_0}{(1-C_3)\gamma\Phi\theta_9V_0} \right) \Psi_{I_1} \\ + (1-C_6)\Phi\theta_9S_1\Psi_{S_1} + (1-C_7)\gamma\Phi\theta_9V_1\Psi_{V_1} - ((1-C_6)\Phi\theta_9S_1 + (1-C_7)\gamma\Phi\theta_9V_1)\Psi_{I_2} + (1-C_{10})\Phi\theta_9S_2\Psi_{S_2} \\ + (1-C_{11})\gamma\Phi\theta_9V_2\Psi_{V_2} - ((1-C_{10})\Phi\theta_9S_2 + (1-C_{11})\gamma\Phi\theta_9V_2)\Psi_{I_3} + (\tau_2 + \mu + \delta)\Psi_{H_3} - \tau_2\Psi_{R_3} \end{array} \right] \quad (36)$$

$$\frac{d\Psi_{R_3}}{dt} = -\frac{\partial H}{dR_3} = \left[-T_1 + ((1-C_{13})\psi + \mu)\Psi_{R_3} - (1-C_{13})\psi\Psi_{S_2} \right] \quad (37)$$

Given the conditions of transversally to be

$$\Psi_i, i \in \{M, S_0, V_0, I_1, H_1, R_1, S_1, V_1, I_2, H_2, R_2, S_2, V_3, I_3, H_3, R_3\}.$$

In pursuit of minimizing the Hamiltonian, denoted as H, in relation to the optimal control variables, we undertake the process of differentiation concerning

$C = C_1, C_2, C_3, C_4, C_5, C_6, C_7, C_8, C_9, C_{10}, C_{11}, C_{12}, C_{13}$. By doing so, we derive a set of equations, which we subsequently set to zero to solve for the optimal control configuration. This procedure yields the sought-after optimal control solution.

Taking $M = M^*, S_0 = S_0^*, V_0 = V_0^*, I_1 = I_1^*, H_1 = H_1^*, R_1 = R_1^*, S_1 = S_1^*, V_1 = V_1^*, I_2 = I_2^*, H_2 = H_2^*, R_2 = R_2^*, S_2 = S_2^*, V_3 = V_3^*, I_3 = I_3^*, H_3 = H_3^*, R_3 = R_3^*$

$$G = T_1R_3 + T_2H_3 + T_3V_2 + T_4S_2 + T_5R_2 + T_6H_2 + T_7V_1 + T_8S_1 + T_9R_1 + T_{10}H_1 + T_{11}V_0 + T_{12}S_0 + T_{13}M + \frac{1}{2}(U)$$

Where $U = U_1C_1^2 + U_2C_2^2 + U_3C_3^2 + U_4C_4^2 + U_5C_5^2 + U_6C_6^2 + U_7C_7^2 + U_8C_8^2 + U_9C_9^2 + U_{10}C_{10}^2 + U_{11}C_{11}^2 + U_{12}C_{12}^2 + U_{13}C_{13}^2$

$$\frac{dH}{dC_1} = U_1C_1^* - (\eta(\Phi\theta_1M + \Lambda) + 1)\Psi_M - \Psi_{V_0} + \eta(\Phi\theta_1M + \Lambda)\Psi_{I_1} - \eta\Phi\theta_2M\Psi_M + \eta\Phi\theta_2M\Psi_{I_1} \quad (38)$$

$$- \eta\Phi\theta_3M\Psi_M + \eta\Phi\theta_3M\Psi_{I_1} - \eta\Phi\theta_4M\Psi_M + \eta\Phi\theta_4M\Psi_{I_1} - \eta\Phi\theta_5M\Psi_M + \eta\Phi\theta_5M\Psi_{I_1} - \eta\Phi\theta_6M\Psi_M + \eta\Phi\theta_6M\Psi_{I_1} - \eta\Phi\theta_7M\Psi_M + \eta\Phi\theta_7M\Psi_{I_1} - \eta\Phi\theta_8M\Psi_M + \eta\Phi\theta_8M\Psi_{I_1} - \eta\Phi\theta_9M\Psi_M + \eta\Phi\theta_9M\Psi_{I_1} = 0$$

$$\frac{dH}{dC_2} = U_2C_2^* - \Phi\theta_1S_0\Psi_{S_0} + \Phi\theta_1S_0\Psi_{I_1} - (\Lambda - 1)\Psi_{S_0} - \Psi_{V_0} + \Lambda\Psi_{I_1} - \Phi\theta_2S_0\Psi_{S_0} + \Phi\theta_2S_0\Psi_{I_1} - \Phi\theta_3S_0\Psi_{S_0} + \Phi\theta_3S_0\Psi_{I_1} - \Phi\theta_4S_0\Psi_{S_0} + \Phi\theta_4S_0\Psi_{I_1} - \Phi\theta_5S_0\Psi_{S_0} + \Phi\theta_5S_0\Psi_{I_1} - \Phi\theta_6S_0\Psi_{S_0} + \Phi\theta_6S_0\Psi_{I_1} - \Phi\theta_7S_0\Psi_{S_0} + \Phi\theta_7S_0\Psi_{I_1} - \Phi\theta_8S_0\Psi_{S_0} + \Phi\theta_8S_0\Psi_{I_1} - \Phi\theta_9S_0\Psi_{S_0} + \Phi\theta_9S_0\Psi_{I_1} = 0 \quad (39)$$

$$\frac{dH}{dC_3} = U_3C_3^* - \gamma\Phi\theta_1V_0\Psi_{V_0} + \gamma\Phi\theta_1V_0\Psi_{I_1} - \gamma(\Phi\theta_2V_0 + \Lambda)\Psi_{V_0} + \gamma(\Phi\theta_2V_0 + \Lambda)\Psi_{I_1} - \gamma\Phi\theta_3V_0\Psi_{V_0} + \gamma\Phi\theta_3V_0\Psi_{I_1} - \gamma\Phi\theta_4V_0\Psi_{V_0} + \gamma\Phi\theta_4V_0\Psi_{I_1} - \gamma\Phi\theta_5V_0\Psi_{V_0} + \gamma\Phi\theta_5V_0\Psi_{I_1} - \gamma\Phi\theta_6V_0\Psi_{V_0} + \gamma\Phi\theta_6V_0\Psi_{I_1} - \gamma\Phi\theta_7V_0\Psi_{V_0} + \gamma\Phi\theta_7V_0\Psi_{I_1} - \gamma\Phi\theta_8V_0\Psi_{V_0} + \gamma\Phi\theta_8V_0\Psi_{I_1} - \gamma\Phi\theta_9V_0\Psi_{V_0} + \gamma\Phi\theta_9V_0\Psi_{I_1} = 0 \quad (40)$$

$$\frac{dH}{dC_4} = U_4C_4^* - \Psi_{I_1} - \Psi_{H_1} = 0 \quad (41)$$

$$\frac{dH}{dC_5} = U_5C_5^* - \psi\Psi_{R_1} + \psi\Psi_{S_1} = 0 \quad (42)$$

$$\begin{aligned} \frac{dH}{dC_6} = & U_6 C_6^* - \Phi \theta_1 S_1 \Psi_{S_1} + \Phi \theta_1 S_1 \Psi_{I_2} - \Phi \theta_2 S_1 \Psi_{S_1} + \Phi \theta_2 S_1 \Psi_{I_2} - \Phi S_1 \Psi_{S_1} + \Phi S_1 \Psi_{I_2} - \Phi \theta_3 S_1 \Psi_{S_1} + \Phi \theta_3 S_1 \Psi_{I_2} \\ & - (\Lambda - 1) \Psi_{S_1} - \Psi_{V_1} + \Lambda \Psi_{I_2} - \Phi \theta_4 S_1 \Psi_{S_1} + \Phi \theta_4 S_1 \Psi_{I_2} - \Phi \theta_5 S_1 \Psi_{S_1} + \Phi \theta_5 S_1 \Psi_{I_2} - \Phi \theta_6 S_1 \Psi_{S_1} + \Phi \theta_6 S_1 \Psi_{I_2} \\ & - \Phi \theta_7 S_1 \Psi_{S_1} + \Phi \theta_7 S_1 \Psi_{I_2} - \Phi \theta_8 S_1 \Psi_{S_1} + \Phi \theta_8 S_1 \Psi_{I_2} - \Phi \theta_9 S_1 \Psi_{S_1} + \Phi \theta_9 S_1 \Psi_{I_2} = 0 \end{aligned} \quad (43)$$

$$\begin{aligned} \frac{dH}{dC_7} = & U_7 C_7^* - \gamma \Phi \theta_1 V_1 \Psi_{V_1} + \gamma \Phi \theta_1 V_1 \Psi_{I_2} - \gamma \Phi \theta_2 V_1 \Psi_{V_1} + \gamma \Phi \theta_2 V_1 \Psi_{I_2} - \gamma \Phi V_1 \Psi_{V_1} + \gamma \Phi V_1 \Psi_{I_2} - \gamma \Phi \theta_3 V_1 \Psi_{V_1} \\ & + \gamma \Phi \theta_3 V_1 \Psi_{I_2} - \gamma (\Phi \theta_4 V_1 + \Lambda) \Psi_{V_1} + \gamma (\Phi \theta_4 V_1 + \Lambda) \Psi_{I_2} - \gamma \Phi \theta_5 V_1 \Psi_{V_1} + \gamma \Phi \theta_5 V_1 \Psi_{I_2} - \gamma \Phi \theta_6 V_1 \Psi_{V_1} + \gamma \Phi \theta_6 V_1 \Psi_{I_2} \\ & - \gamma \Phi \theta_7 V_1 \Psi_{V_1} + \gamma \Phi \theta_7 V_1 \Psi_{I_2} - \gamma \Phi \theta_8 V_1 \Psi_{V_1} + \gamma \Phi \theta_8 V_1 \Psi_{I_2} - \gamma \Phi \theta_9 V_1 \Psi_{V_1} + \gamma \Phi \theta_9 V_1 \Psi_{I_2} = 0 \end{aligned} \quad (44)$$

$$\frac{dH}{dC_8} = U_8 C_8^* - \Psi_{I_2} - \Psi_{H_2} = 0 \quad (45)$$

$$\frac{dH}{dC_9} = U_9 C_9^* - \psi \Psi_{R_2} + \psi \Psi_{S_2} = 0 \quad (46)$$

$$\begin{aligned} \frac{dH}{dC_{10}} = & U_{10} C_{10}^* - \Phi \theta_1 S_2 \Psi_{S_2} + \Phi \theta_1 S_2 \Psi_{I_3} - \Phi \theta_2 S_2 \Psi_{S_2} + \Phi \theta_2 S_2 \Psi_{I_3} - \Phi S_2 \Psi_{S_2} + \Phi S_2 \Psi_{I_3} - \Phi \theta_3 S_2 \Psi_{S_2} + \Phi \theta_3 S_2 \Psi_{I_3} \\ & - \Phi \theta_4 S_2 \Psi_{S_2} + \Phi \theta_4 S_2 \Psi_{I_3} - \Phi \theta_5 S_2 \Psi_{S_2} + \Phi \theta_5 S_2 \Psi_{I_3} - \Phi \theta_6 S_2 \Psi_{S_2} + \Phi \theta_6 S_2 \Psi_{I_3} - (\Lambda - 1) \Psi_{S_2} - \Psi_{V_2} + \Lambda \Psi_{I_3} \\ & - \Phi \theta_7 S_2 \Psi_{S_2} + \Phi \theta_7 S_2 \Psi_{I_3} - \Phi \theta_8 S_2 \Psi_{S_2} + \Phi \theta_8 S_2 \Psi_{I_3} - \Phi \theta_9 S_2 \Psi_{S_2} + \Phi \theta_9 S_2 \Psi_{I_3} = 0 \end{aligned} \quad (47)$$

$$\begin{aligned} \frac{dH}{dC_{11}} = & U_{11} C_{11}^* - \gamma \Phi \theta_1 V_2 \Psi_{V_2} + \gamma \Phi \theta_1 V_2 \Psi_{I_3} - \gamma \Phi \theta_2 V_2 \Psi_{V_2} + \gamma \Phi \theta_2 V_2 \Psi_{I_3} - \gamma \Phi V_2 \Psi_{V_2} + \gamma \Phi V_2 \Psi_{I_3} - \gamma \Phi \theta_3 V_2 \Psi_{V_2} \\ & + \gamma \Phi \theta_3 V_2 \Psi_{I_3} - \gamma \Phi \theta_4 V_2 \Psi_{V_2} + \gamma \Phi \theta_4 V_2 \Psi_{I_3} - \gamma \Phi \theta_5 V_2 \Psi_{V_2} + \gamma \Phi \theta_5 V_2 \Psi_{I_3} - \gamma (\Phi \theta_6 V_2 + \Lambda) \Psi_{V_2} + \gamma (\Phi \theta_6 V_2 + \Lambda) \Psi_{I_3} \\ & - \gamma \Phi \theta_7 V_2 \Psi_{V_2} + \gamma \Phi \theta_7 V_2 \Psi_{I_3} - \gamma \Phi \theta_8 V_2 \Psi_{V_2} + \gamma \Phi \theta_8 V_2 \Psi_{I_3} - \gamma \Phi \theta_9 V_2 \Psi_{V_2} + \gamma \Phi \theta_9 V_2 \Psi_{I_3} = 0 \end{aligned} \quad (48)$$

$$\frac{dH}{dC_{12}} = U_{12} C_{12}^* - \Psi_{I_3} - \Psi_{H_3} = 0 \quad (49)$$

$$\frac{dH}{dC_{13}} = U_{13} C_{13}^* - \psi \Psi_{R_{13}} + \psi \Psi_{S_{12}} = 0 \quad (50)$$

By simplification, we obtain a solution for the optimal control to be

$$C_1^* = \frac{\left[\begin{aligned} & (\eta(\Phi \theta_1 M + \Lambda) + 1) \Psi_M + \Psi_{V_0} - \eta(\Phi \theta_1 M + \Lambda) \Psi_{I_1} + \eta \Phi \theta_2 M \Psi_M - \Phi \theta_2 M \Psi_{I_1} + \eta \Phi M \Psi_M - \eta \Phi M \Psi_{I_1} \\ & + \eta \Phi \theta_3 M \Psi_M - \eta \Phi \theta_3 M \Psi_{I_1} + \eta \Phi \theta_4 M \Psi_M - \eta \Phi \theta_4 M \Psi_{I_1} + \eta \Phi \theta_5 M \Psi_M - \eta \Phi \theta_5 M \Psi_{I_1} + \eta \Phi \theta_6 M \Psi_M \\ & - \eta \Phi \theta_6 M \Psi_{I_1} + \eta \Phi \theta_7 M \Psi_M - \eta \Phi \theta_7 M \Psi_{I_1} + \eta \Phi \theta_8 M \Psi_M - \eta \Phi \theta_8 M \Psi_{I_1} + \eta \Phi \theta_9 M \Psi_M - \eta \Phi \theta_9 M \Psi_{I_1} \end{aligned} \right]}{U_1} \quad (51)$$

$$C_2^* = \frac{\left[\begin{aligned} & \Phi \theta_1 S_0 \Psi_{S_0} - \Phi \theta_1 S_0 \Psi_{I_1} + (\Lambda - 1) \Psi_{S_0} + \Psi_{V_0} - \Lambda \Psi_{I_1} + \Phi \theta_2 S_0 \Psi_{S_0} - \Phi \theta_2 S_0 \Psi_{I_1} + \Phi S_0 \Psi_{S_0} - \Phi S_0 \Psi_{I_1} \\ & + \Phi \theta_3 S_0 \Psi_{S_0} - \Phi \theta_3 S_0 \Psi_{I_1} + \Phi \theta_4 S_0 \Psi_{S_0} - \Phi \theta_4 S_0 \Psi_{I_1} + \Phi \theta_5 S_0 \Psi_{S_0} - \Phi \theta_5 S_0 \Psi_{I_1} + \Phi \theta_6 S_0 \Psi_{S_0} \\ & - \Phi \theta_6 S_0 \Psi_{I_1} + \Phi \theta_7 S_0 \Psi_{S_0} - \Phi \theta_7 S_0 \Psi_{I_1} + \Phi \theta_8 S_0 \Psi_{S_0} - \Phi \theta_8 S_0 \Psi_{I_1} + \Phi \theta_9 S_0 \Psi_{S_0} - \Phi \theta_9 S_0 \Psi_{I_1} \end{aligned} \right]}{U_2} \quad (52)$$

$$C_3^* = \frac{\left[\begin{aligned} & \gamma \Phi \theta_1 V_0 \Psi_{V_0} - \gamma \Phi \theta_1 V_0 \Psi_{I_1} + \gamma (\Phi \theta_2 V_0 + \Lambda) \Psi_{V_0} - \gamma (\Phi \theta_2 V_0 + \Lambda) \Psi_{I_1} + \gamma \Phi V_0 \Psi_{V_0} - \gamma \Phi V_0 \Psi_{I_1} + \gamma \Phi \theta_3 V_0 \Psi_{V_0} \\ & - \gamma \Phi \theta_3 V_0 \Psi_{I_1} + \gamma \Phi \theta_4 V_0 \Psi_{V_0} - \gamma \Phi \theta_4 V_0 \Psi_{I_1} + \gamma \Phi \theta_5 V_0 \Psi_{V_0} - \gamma \Phi \theta_5 V_0 \Psi_{I_1} + \gamma \Phi \theta_6 V_0 \Psi_{V_0} - \gamma \Phi \theta_6 V_0 \Psi_{I_1} + \gamma \Phi \theta_7 V_0 \Psi_{V_0} \\ & - \gamma \Phi \theta_7 V_0 \Psi_{I_1} + \gamma \Phi \theta_8 V_0 \Psi_{V_0} - \Phi \theta_8 \gamma V_0 \Psi_{I_1} + \gamma \Phi \theta_9 V_0 \Psi_{V_0} - \Phi \theta_9 \gamma V_0 \Psi_{I_1} \end{aligned} \right]}{U_3} \quad (53)$$

$$C_4^* = \frac{\Psi_{I_1} + \Psi_{H_1}}{U_4} \quad (54)$$

$$C_5^* = \frac{\psi(\Psi_{R_1} - \Psi_{S_1})}{U_5} \quad (55)$$

$$C_6^* = \frac{\left[\begin{aligned} &\Phi\theta_1 S_1 \Psi_{S_1} - \Phi\theta_1 S_1 \Psi_{I_2} + \Phi\theta_2 S_1 \Psi_{S_1} - \Phi\theta_2 S_1 \Psi_{I_2} + \Phi S_1 \Psi_{S_1} - \Phi S_1 \Psi_{I_2} + \Phi\theta_3 S_1 \Psi_{S_1} - \Phi\theta_3 S_1 \Psi_{I_2} \\ &+ (\Lambda - 1)\Psi_{S_1} + \Psi_{V_1} - \Lambda\Psi_{I_2} + \Phi\theta_4 S_1 \Psi_{S_1} - \Phi\theta_4 S_1 \Psi_{I_2} + \Phi\theta_5 S_1 \Psi_{S_1} - \Phi\theta_5 S_1 \Psi_{I_2} + \Phi\theta_6 S_1 \Psi_{S_1} - \Phi\theta_6 S_1 \Psi_{I_2} \\ &+ \Phi\theta_7 S_1 \Psi_{S_1} - \Phi\theta_7 S_1 \Psi_{I_2} + \Phi\theta_8 S_1 \Psi_{S_1} - \Phi\theta_8 S_1 \Psi_{I_2} + \Phi\theta_9 S_1 \Psi_{S_1} - \Phi\theta_9 S_1 \Psi_{I_2} \end{aligned} \right]}{U_6} \quad (56)$$

$$C_7^* = \frac{\left[\begin{aligned} &\gamma\Phi\theta_1 V_1 \Psi_{V_1} - \gamma\Phi\theta_1 V_1 \Psi_{I_2} + \gamma\Phi\theta_2 V_1 \Psi_{V_1} - \gamma\Phi\theta_2 V_1 \Psi_{I_2} + \gamma\Phi V_1 \Psi_{V_1} - \gamma\Phi V_1 \Psi_{I_2} + \gamma\Phi\theta_3 V_1 \Psi_{V_1} \\ &- \gamma\Phi\theta_3 V_1 \Psi_{I_2} + \gamma(\Phi\theta_4 V_1 + \Lambda)\Psi_{V_1} - \gamma(\Phi\theta_4 V_1 + \Lambda)\Psi_{I_2} + \gamma\Phi\theta_5 V_1 \Psi_{V_1} - \gamma\Phi\theta_5 V_1 \Psi_{I_2} + \gamma\Phi\theta_6 V_1 \Psi_{V_1} \\ &- \gamma\Phi\theta_6 V_1 \Psi_{I_2} + \gamma\Phi\theta_7 V_1 \Psi_{V_1} - \gamma\Phi\theta_7 V_1 \Psi_{I_2} + \gamma\Phi\theta_8 V_1 \Psi_{V_1} - \gamma\Phi\theta_8 V_1 \Psi_{I_2} + \gamma\Phi\theta_9 V_1 \Psi_{V_1} - \gamma\Phi\theta_9 V_1 \Psi_{I_2} \end{aligned} \right]}{U_7} \quad (57)$$

$$C_8^* = \frac{\Psi_{I_2} + \Psi_{H_2}}{U_8} \quad (58)$$

$$C_9^* = \frac{\psi(\Psi_{R_2} - \Psi_{S_2})}{U_9} \quad (59)$$

$$C_{10}^* = \frac{\left[\begin{aligned} &\Phi\theta_1 S_2 \Psi_{S_2} - \Phi\theta_1 S_2 \Psi_{I_3} + \Phi\theta_2 S_2 \Psi_{S_2} - \Phi\theta_2 S_2 \Psi_{I_3} + \Phi S_2 \Psi_{S_2} - \Phi S_2 \Psi_{I_3} + \Phi\theta_3 S_2 \Psi_{S_2} - \Phi\theta_3 S_2 \Psi_{I_3} \\ &+ \Phi\theta_4 S_2 \Psi_{S_2} - \Phi\theta_4 S_2 \Psi_{I_3} + \Phi\theta_5 S_2 \Psi_{S_2} - \Phi\theta_5 S_2 \Psi_{I_3} + \Phi\theta_6 S_2 \Psi_{S_2} - \Phi\theta_6 S_2 \Psi_{I_3} + (\Lambda - 1)\Psi_{S_2} + \Psi_{V_2} - \Lambda\Psi_{I_3} \\ &+ \Phi\theta_7 S_2 \Psi_{S_2} - \Phi\theta_7 S_2 \Psi_{I_3} + \Phi\theta_8 S_2 \Psi_{S_2} - \Phi\theta_8 S_2 \Psi_{I_3} + \Phi\theta_9 S_2 \Psi_{S_2} - \Phi\theta_9 S_2 \Psi_{I_3} \end{aligned} \right]}{U_{10}} \quad (60)$$

$$C_{11}^* = \frac{\left[\begin{aligned} &\gamma\Phi\theta_1 V_2 \Psi_{V_2} - \gamma\Phi\theta_1 V_2 \Psi_{I_3} + \gamma\Phi\theta_2 V_2 \Psi_{V_2} - \gamma\Phi\theta_2 V_2 \Psi_{I_3} + \gamma\Phi V_2 \Psi_{V_2} - \gamma\Phi V_2 \Psi_{I_3} + \gamma\Phi\theta_3 V_2 \Psi_{V_2} \\ &- \gamma\Phi\theta_3 V_2 \Psi_{I_3} + \gamma\Phi\theta_5 V_2 \Psi_{V_2} - \gamma\Phi\theta_5 V_2 \Psi_{I_3} + \gamma\Phi\theta_6 V_2 \Psi_{V_2} - \gamma\Phi\theta_6 V_2 \Psi_{I_3} + \gamma(\Phi\theta_7 V_2 + \Lambda)\Psi_{V_2} \\ &- \gamma(\Phi\theta_7 V_2 + \Lambda)\Psi_{I_3} + \gamma\Phi\theta_8 V_2 \Psi_{V_2} - \gamma\Phi\theta_8 V_2 \Psi_{I_3} + \gamma\Phi\theta_9 V_2 \Psi_{V_2} - \gamma\Phi\theta_9 V_2 \Psi_{I_3} \end{aligned} \right]}{U_{11}} \quad (61)$$

$$C_{12}^* = \frac{\Psi_{I_3} + \Psi_{H_3}}{U_{12}} \quad (62)$$

$$C_{13}^* = \frac{\psi(\Psi_{R_3} - \Psi_{S_2})}{U_{13}} \quad (63)$$

Now, making use of the boundary conditions, the solution given has

$$\begin{aligned} C_1 &= \min \{1, \max \{0, C_1^*\}\}; C_2 = \min \{1, \max \{0, C_2^*\}\}; C_3 = \min \{1, \max \{0, C_3^*\}\}, \\ C_4 &= \min \{1, \max \{0, C_4^*\}\}; C_5 = \min \{1, \max \{0, C_5^*\}\}; C_6 = \min \{1, \max \{0, C_6^*\}\}, \\ C_7 &= \min \{1, \max \{0, C_7^*\}\}; C_8 = \min \{1, \max \{0, C_8^*\}\}; C_9 = \min \{1, \max \{0, C_9^*\}\}, \\ C_{10} &= \min \{1, \max \{0, C_{10}^*\}\}; C_{11} = \min \{1, \max \{0, C_{11}^*\}\}; C_{12} = \min \{1, \max \{0, C_{12}^*\}\}, \\ C_{13} &= \min \{1, \max \{0, C_{13}^*\}\}; \end{aligned} \quad (64)$$

And Where $\Lambda = \Phi(I_1 + \theta_1 M + \theta_2 V_0 + \theta_3 H_1 + \theta_4 V_1 + \theta_5 I_2 + \theta_6 H_2 + \theta_7 V_2 + \theta_8 I_3 + \theta_9 H_3)$

Results

In this simulation, we offer a means to observe the progression of the disease over time, track alterations in various parameters, and evaluate the effectiveness of interventions. This platform enables researchers and public health authorities to acquire valuable insights into the disease's behaviour across different scenarios and to assess the efficacy of diverse control tactics.

The state variables' initial conditions are as follows: $M = 150$, $S_0 = 200$, $V_0 = 100$, $I_1 = 200$, $H_1 = 250$, $R_1 = 200$, $S_1 = 190$, $V_1 = 150$, $I_2 = 150$, $H_2 = 140$, $R_2 = 130$, $S_2 = 120$, $V_2 = 100$, $I_3 = 110$, $H_3 = 100$, and $R_3 = 90$. Also, $\xi = 0.5$; $\eta = 0.62$; $\kappa = 0.333$; $\rho = 0.3$; $\theta_1 = 0.62$; $\theta_2 = 0.62$; $\theta_4 = 0.35$; $\tau_1 = 8.6$; $\tau_2 = 8.6$; $\gamma = 0.71$; $\psi = 0.083$; $\theta_5 = 0.5$; $\theta_6 = 0.5$; $\theta_7 = 0.5$; $\theta_8 = 0.1$; The parameter values needed for the simulation are displayed in Table 2 above.

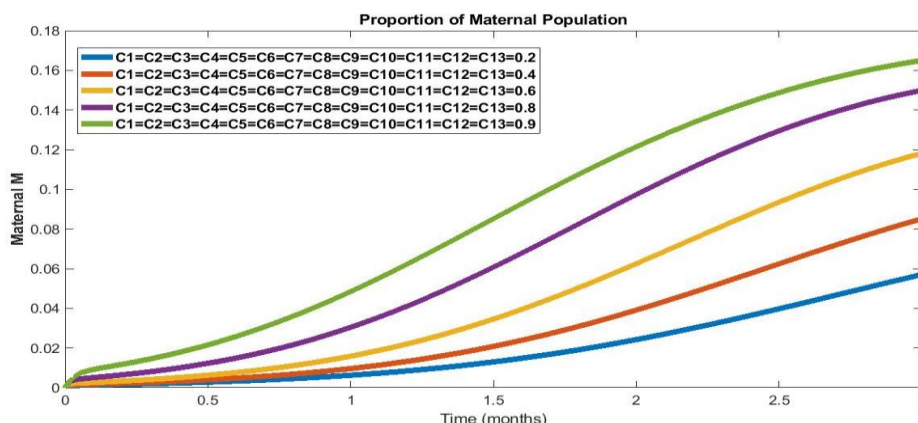


Figure 4: Trajectories for optimizing maternal control

Discussion

Figure 4 illustrates that an increase in the application of the specified control strategies for rotavirus corresponds to a noticeable boost in the immunity of individuals during maternal care. In simpler terms, when these control measures are effectively employed, there is a positive relationship with enhanced immunity levels in individuals receiving maternal care. This implies that the aforementioned strategies- prenatal education, vaccination, isolation, medical care, infection control, and immunity monitoring- all contribute to improved immunity outcomes in individuals during maternal care. Figure 4 visually represents this favorable association between the usage of control strategies and the increase in maternal immunity.

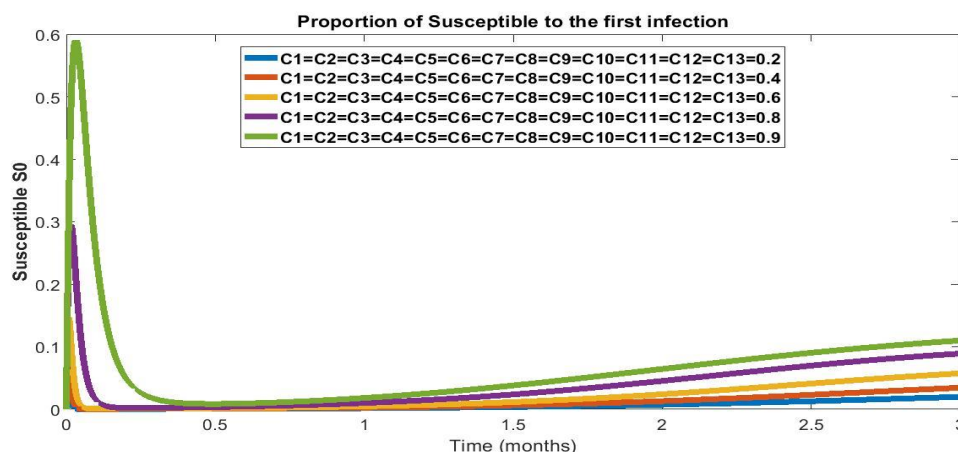


Figure 5: Trajectories for optimizing susceptibility to the first infection control

Figure 5 demonstrates that as the utilization of the control strategies described in the earlier statements increases, the number of individuals susceptible to the first infection also rises. Put differently, the more efficiently these control strategies are implemented, the greater the number of individuals who remain susceptible to the first infection due to a lower initial infection rate. This suggests that the control measures effectively reduce the incidence of the first infection, resulting in a larger pool of individuals who have not yet been exposed.

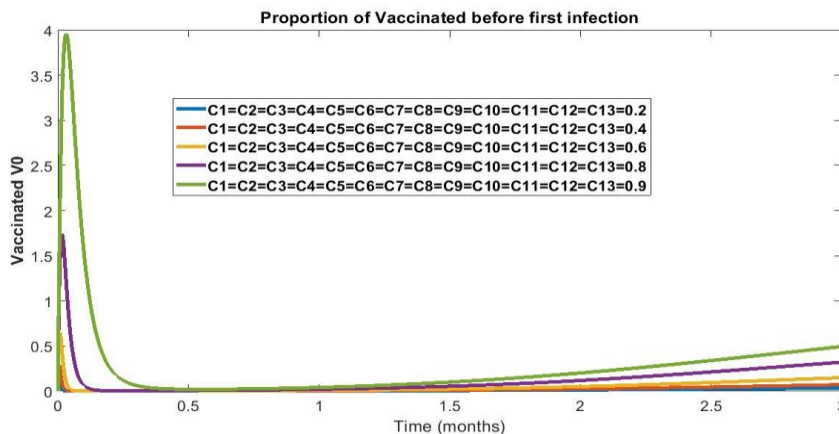


Figure 6: Trajectories for optimizing vaccination before the first infection control

Figure 6 reveals that as the usage of the mentioned control strategies increases, the number of individuals vaccinated before experiencing their first rotavirus infection also rises. In other words, the implementation of these control measures is associated with a higher rate of individuals receiving vaccination before encountering the virus for the first time. This indicates that the strategies effectively promote vaccination and, consequently, reduce the risk of rotavirus infection in the population.

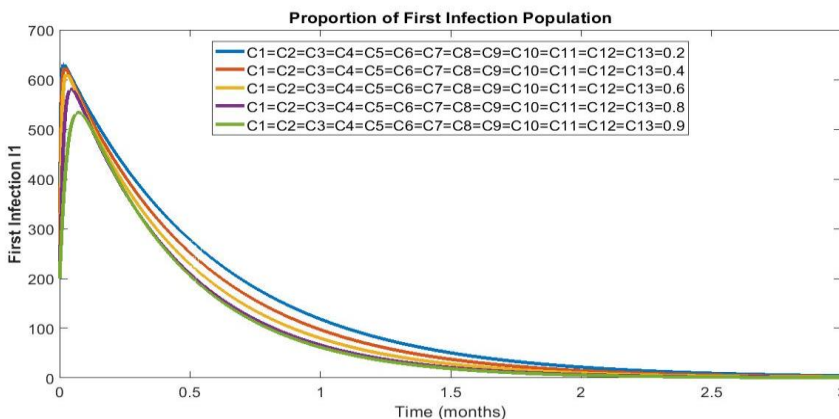


Figure 7: Trajectories for optimizing first infection population control

Figure 7 shows that the implementation of the control strategies mentioned earlier leads to a decrease in the number of individuals in the population experiencing the first infection, as depicted in Figure 7. In simpler terms, as more people adhere to recommended measures such as vaccination, isolation, medical care, infection control, and immunity monitoring, the occurrence of initial rotavirus infections diminishes, as visually represented in Figure 7. This suggests that these control strategies are effective in reducing the incidence of initial rotavirus infections.

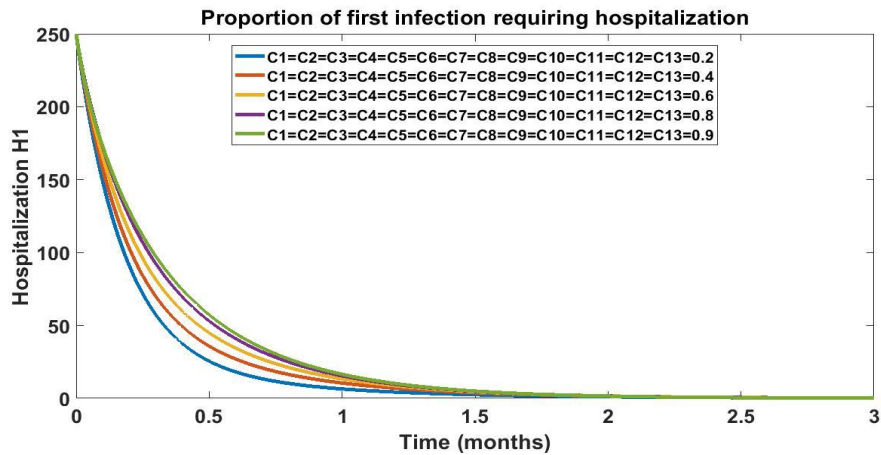


Figure 8: Trajectories for optimizing of first infection requiring hospitalization control

Figure 8 indicates that as the utilization of the control strategies mentioned in the previous statements increases, the number of individuals requiring hospitalization after their first rotavirus infection also rises. In other words, there appears to be a correlation between the implementation of these control measures and the hospitalization rate for individuals experiencing their initial rotavirus infection.

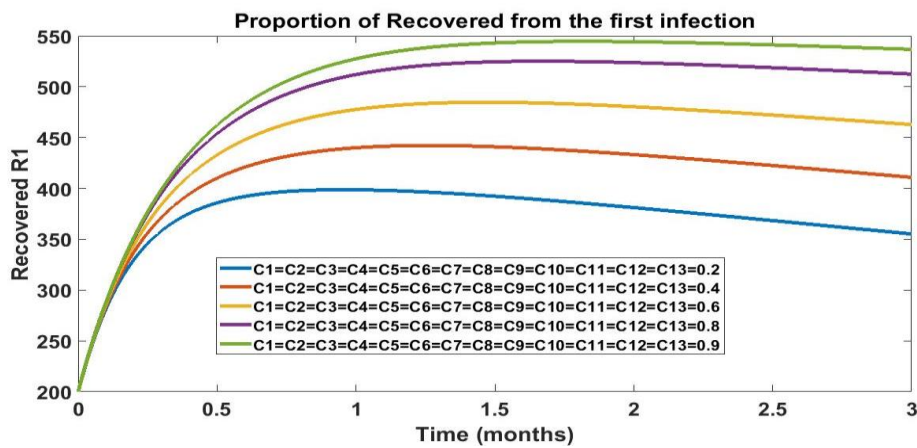


Figure 9: Trajectories for optimizing recovery from the first infection control

Figure 9 suggests that as the utilization of the mentioned control strategies for rotavirus increases, the number of individuals who have recovered from the first infection also rises, as shown in Figure 9. In simpler terms, the effective implementation of these control measures is associated with a higher rate of recovery from the initial rotavirus infection.

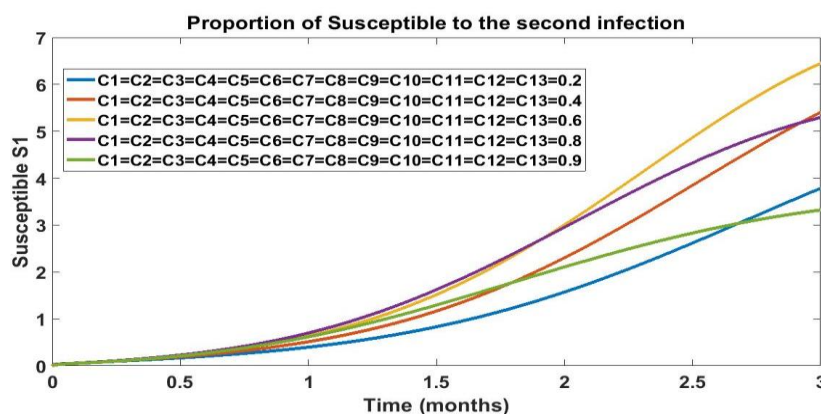


Figure 10: Trajectories for optimizing susceptibility to the second infection control

Figure 10 suggests a relationship between the usage of control strategies for rotavirus and individuals' susceptibility to a second infection. Specifically, as the usage of these control strategies increases from 0.2 to 0.6, the number of individuals susceptible to a second infection also rises. However, when the usage of these control

strategies further increases from 0.8 to 0.9, the number of susceptible individuals starts to decrease. In simpler terms, it appears that there is an optimal range of control strategy usage (between 0.6 and 0.8) where susceptibility to a second rotavirus infection is minimized. Beyond this optimal range, increasing the usage of control strategies may not have as significant an impact on reducing susceptibility or may even yield diminishing returns.

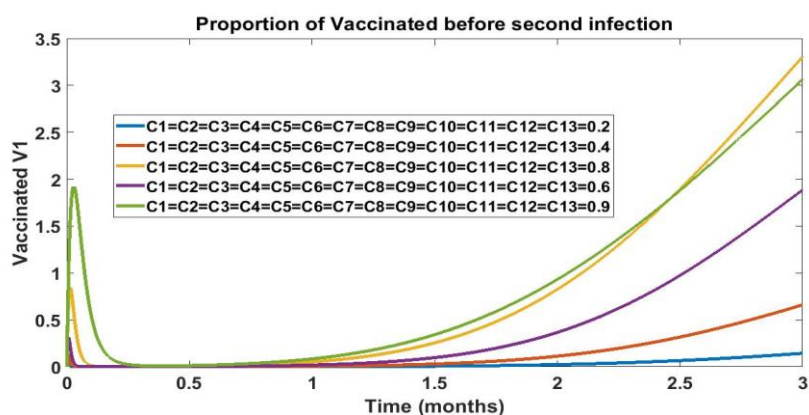


Figure 11: Trajectories for optimizing vaccination before the second infection control

Figure 11 suggests a relationship between the usage of control strategies for rotavirus and the number of individuals vaccinated before experiencing their second infection. Specifically, when control strategy usage increases from 0.2 to 0.6, the number of individuals vaccinated before their second infection also rises. However, after reaching a certain point (when control strategy usage increases from 0.8 to 0.9), the number of individuals being vaccinated before their second infection starts to decrease. This indicates that there might be an optimal range or threshold of control strategy usage beyond which the effectiveness of vaccination in preventing second infections decreases or becomes less efficient.

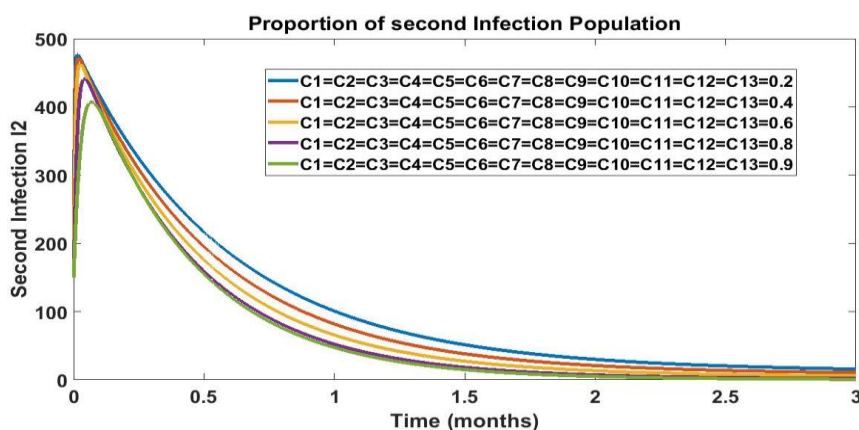


Figure 12: Trajectories for optimizing second infection population control

Figure 12 suggests that as the utilization of the mentioned control strategies increases, the proportion of the population experiencing a second infection with rotavirus decreases, as illustrated in Figure 12. In simpler terms, the more effectively these control measures are applied, the lower the likelihood of individuals getting infected for the second time with rotavirus.

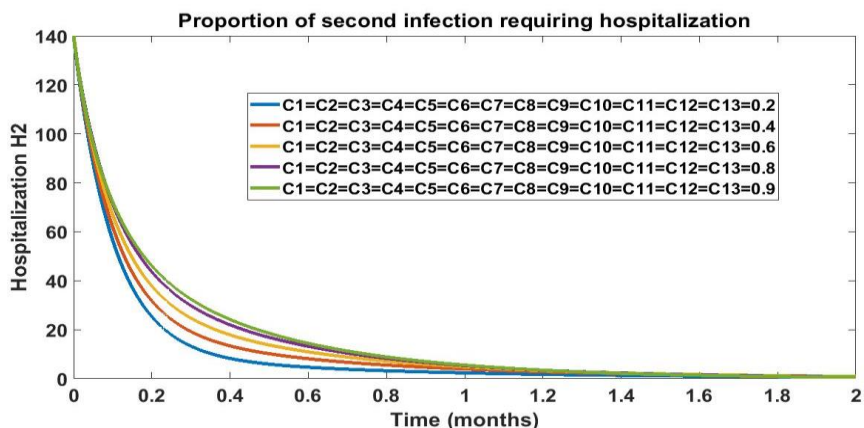


Figure 13: Trajectories for optimizing the second infection requiring hospitalization control
 Figure 13 suggests that as the utilization of the specified control strategies increases, the number of individuals who are hospitalized after experiencing a second infection with rotavirus also rises, as indicated in Figure 13.

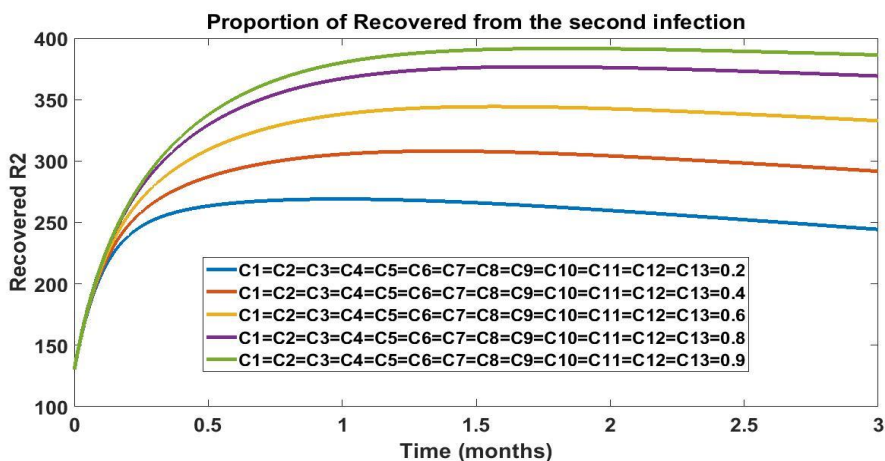


Figure 14: Trajectories for optimizing recovery from the second infection control
 Figure 14 suggests that as the utilization of the control strategies outlined in the previous statements increases, the number of individuals who have recovered from a second infection with rotavirus also increases. In other words, the more effectively these control strategies are implemented, the better the outcome in terms of reducing the number of people who experience a second infection and subsequently recover from it. Figure 14 likely illustrates this relationship visually, demonstrating a positive correlation between the use of control measures and the recovery of individuals from a second rotavirus infection.

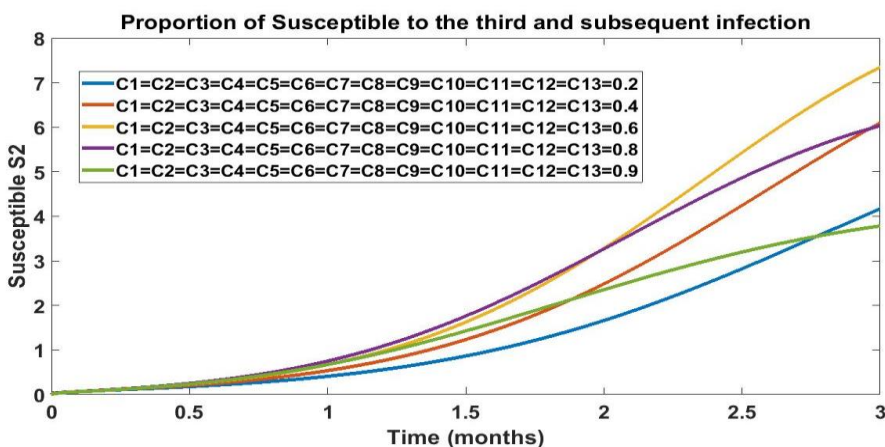


Figure 15: Trajectories for optimizing susceptibility to the third and subsequent infection control

Figure 15 suggests that the effectiveness of the control strategies for rotavirus infections is reflected in the susceptibility of individuals to third and subsequent infections. When the control strategies are used at a level between 0.2 and 0.6, the number of individuals susceptible to third and subsequent infections increases. However, when the usage of these control strategies is increased further, from 0.8 to 0.9, the number of susceptible individuals starts to decrease after 2 months. This implies that there is an optimal range of control strategy usage, between 0.2 and 0.6, where the strategies are most effective at reducing susceptibility to repeat infections. Beyond this optimal range, increasing the usage of the strategies may not yield additional benefits, and in fact, it may lead to a decrease in susceptibility.

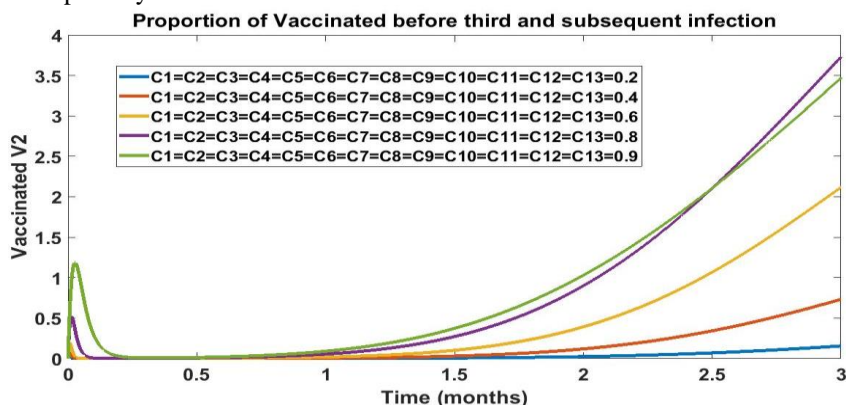


Figure 16: Trajectories for optimizing vaccination before the third and subsequent infection control

Figure 16 indicates that there is a relationship between the usage of control strategies for rotavirus and the number of individuals who are vaccinated before the third and subsequent infections. When the usage of these control strategies increases from 0.2 to 0.6, the number of vaccinated individuals also increases. However, after reaching a certain point (when the control strategies usage increases from 0.8 to 0.9), the number of vaccinated individuals starts to decrease after 2 months. This suggests that there may be an optimal range of control strategy usage for maximizing the number of vaccinated individuals before the third and subsequent infections, and exceeding this range could lead to a decline in vaccination rates.

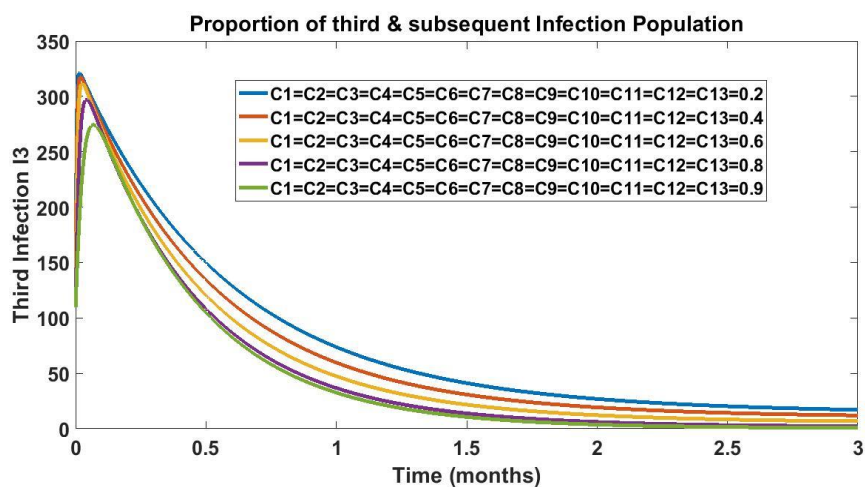


Figure 17: Trajectories for optimizing third and subsequent infection population control

Figure 17 suggests that when the control strategies mentioned earlier are consistently applied, the proportion of individuals experiencing a third or subsequent infection with rotavirus decreases. In simpler terms, by following the recommended actions such as vaccination, isolation, medical care, infection control measures, and immunity monitoring, the incidence of repeated rotavirus infections is reduced. This indicates the effectiveness of these control strategies in preventing multiple infections and improving overall public health outcomes.

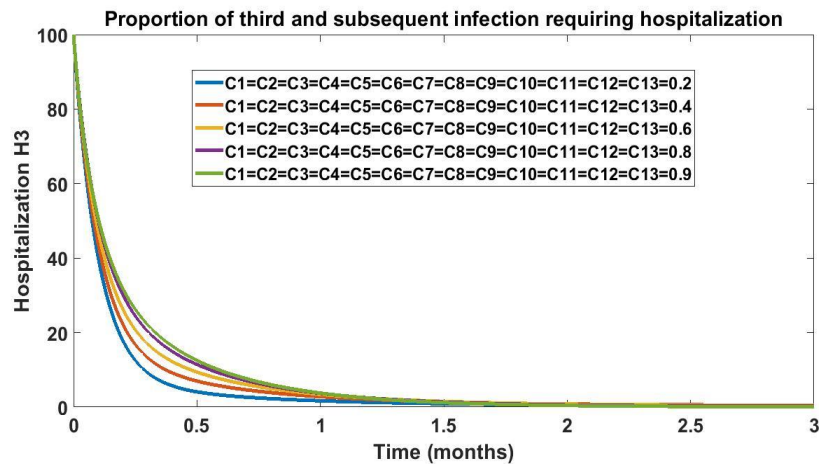


Figure 18: Trajectories for optimizing third and subsequent infection requiring hospitalization control

Figure 18 suggests that as the utilization of the control strategies outlined for rotavirus increases, the number of individuals who are hospitalized after their third and subsequent infections also increases. In other words, there seems to be a correlation between the implementation of these control measures and a rise in hospitalizations for individuals experiencing their third or subsequent infections with rotavirus. This correlation is depicted in Figure 18.

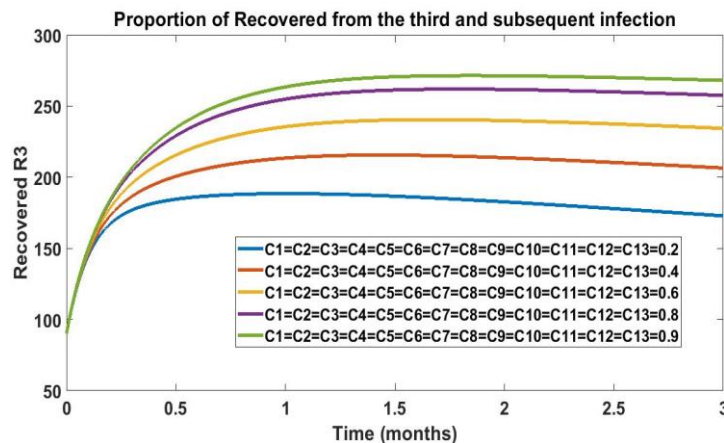


Figure 19: Trajectories for optimizing recovered from the second and subsequent infection control

Figure 19 suggests that as the utilization of the specified control strategies increases, the number of individuals who have recovered from the third and subsequent infections with rotavirus also increases, as indicated in Figure 19. In simpler terms, by implementing these control measures effectively, there is a positive correlation with a higher

Conclusion

Results in Figures 4 to 19 provide a comprehensive overview of the impact of various control strategies on rotavirus infections. For instance, effective implementation of control strategies - prenatal education, vaccination, isolation, medical care, infection control, and immunity monitoring - is associated with increased maternal immunity (Figure 4) and reduced incidence of initial rotavirus infections (Figure 7). These findings underscore the importance of a well-considered approach to control strategies for rotavirus infections. Striking a balance in their implementation, monitoring, and adaptation to changing circumstances can lead to improved immunity, reduced infection rates, and better health outcomes for affected individuals and communities.

Acknowledgement

Mrs. Adetoun Loyinmi and my co-author are appreciated for their love and kind heartedness.

References

Agbomola, J. O., & Loyinmi, A. C. (2022a). A Mathematical model for the dynamical behavior

- of Ebola virus transmission In Human-Bat population: Implication of immediate discharge of recovered individuals. *Preprint*. <https://doi.org/10.21203/rs.3.rs-1399224/v1>
- Agbomola, J. O., & Loyinmi, A. C. (2022b). Modelling the impact of some control strategies on the transmission dynamics of Ebola virus in human-bat population: An optimal control analysis, *Heliyon*, 8(12), e12121. <https://doi.org/10.1016/j.heliyon.2022.e12121>
- Darti, I., Suryanto, A., & Ilmi, N. B. (2020). Dynamical behavior of a Rotavirus transmission model with an environmental effect. *AIP Conference proceedings*, 2264 (1). <https://doi.org/10.1063/5.0023487>
- De Blasio BF, Kasymbekova K, Flem E. (2010). Dynamic model of rotavirus transmission and the impact of rotavirus vaccination in Kyrgyzstan, *Vaccine*, 28 (50), 7923-7932. <https://doi.org/10.1016/j.vaccine.2010.09.070>
- Ernest, O., Asare, Mohammad, A., Al-Mamun, George, E., Armah, Benjamin, A., Lopman, Umesh, D., Parashar, Fred, Binka, Virginia, E., & Pitzer (2020). Modelling of rotavirus transmission dynamics and impact of vaccination in Ghana. *Vaccine*, 38(31) 4820-4828. <https://doi.org/10.1016/j.vaccine.2020.05.057>.
- Galen, V., Rolina, D., Van-de, Kasstele, Hahné, J., Susan, J. M., Bruijning-Verhagen, Wallinga, P., & Jacco. (2017). Determinants of Rotavirus Transmission: A Lag Nonlinear Time Series Analysis, *Epidemiology*, 28(4), 503-513. <https://journals.lww.com/epidem/toc/2017/07000>
- Gbodogbe, S. O. (2025). Harmonizing epidemic dynamics: A fractional calculus approach to optimal control strategies for cholera transmission. *Scientific African*, 27. <https://doi.org/10.1016/j.sciaf.2025.e02545>
- Idowu, O. K., & Loyinmi, A. C. (2023a). Qualitative analysis of the transmission dynamics and optimal Control of Covid-19. *EDUCATUM Journal of Science, Mathematics and Technology*. 10(1), 54–70. <https://doi.org/10.37134/ejsmt.vol10.1.7.2023>
- Idowu, K. O., & Loyinmi, A. C. (2023b). Impact of Contaminated surfaces on the transmission dynamics of Corona Virus Disease (Covid-19). *Biomedical Journal of Scientific and Technical Research*. 51(1), 42280–42294. <https://doi.org/10.26717/BJSTR.2023.51.008046>
- Ilmi, N. B., Darti, I., & Suryanto, A. (2020). Dynamical Analysis of a Rotavirus infection model with vaccination and saturation incidence rate. *Journal of Physics: Conference Series*, 1562(1). IOP Publishing. DOI 10.1088/1742-6596/1562/1/012018
- Kraay, A. N. M., Brouwer, A. F., Lin, N., Collender, P. A., Remais, J. V., & Eisenberg, J. N. S. (2018). Modeling environmentally mediated rotavirus transmission: The role of temperature and hydrologic factors, *PNAS*. 115(12), 2782-2790. <https://doi.org/10.1073/pnas.1719579115>
- Lee, T., Kang, J., Ahn, J. G., Truong, D.T.T., Nguyen, T.V., Vinh, T., Ho, Ton, H.T.T., Hoang, P.L., Kim, M.Y., Yeom, J., & Lee, J. (2024). Prediction of effectiveness of universal rotavirus vaccination in Southwestern Vietnam based on a dynamic mathematical model. *Sci Rep* 14, 4273. <https://doi.org/10.1038/s41598-024-54775-6>
- Loyinmi, A. C., & Ijaola, A. L. (2024a). Investigating the effects of some controls measures on the dynamics of diphtheria infection using fractional order model, *Mathematics and Computational Sciences*, 5(4), 26-47. [10.30511/MCS.2024.2032110.1183](https://doi.org/10.30511/MCS.2024.2032110.1183).
- Loyinmi, A. C., & Ijaola, A. L. (2024b). Fractional order model of dynamical behavior and qualitative analysis of Anthrax with infected vector and saturation. *Int. J of Math. Anal. And Modelling*, 7(2), 224-264.
- Loyinmi, A. C., Ajala, A. S., & Alani, L. I. (2024). Analysis of the effect of vaccination, efficient surveillance and treatment on the transmission dynamics of cholera. *Al-Bahir journal for Engineering and Pure Sciences*, 5(2), 94–107. <https://doi.org/10.55810/2313-0083.1070>
- Loyinmi, A. C., & Gbodogbe, S. O. (2024). Mathematical modeling and control strategies for Nipah virus transmission incorporating Bat – to – pig –to – human pathway. *EDUCATUM Journal of Science, Mathematics and Technology*, 11(1), 54-80. <https://doi.org/10.37134/ejsmt.vol11.1.7.2024>
- Loyinmi, A. C., Gbodogbe, S. O., & Idowu, K. O. (2023). On the interaction of the human immune system with foreign body: mathematical modelling approach. *Kathmandu University Journal of Science, Engineering and Technology*. 17(2), 1-17. <https://journals.ku.edu.np/kuset/article/view/137>
- Loyinmi, A. C., Akinfe, T. K., & Ojo, A. A. (2021). Qualitative analysis and dynamical behavior of a Lassa haemorrhagic fever model with exposed rodents and saturated incidence rate. *Scientific African*, 14, e01028. <https://doi.org/10.1016/j.sciaf.2021.e01028>.
- Lopman, B. A., Pitzer, V. E., Sarkar, R., Gladstone, B., Patel, M., & Glasser, J. (2012). Understanding reduced rotavirus vaccine efficacy in low socio-economic settings *PLoS ONE*, 7(8), e41720.

- Margaret, M., Cortese, M. D., & Penina Haber, M.P.H. (2021), Rotavirus, <https://www.scribd.com/document/639432146/Untitled>.
- Park, J., Goldstein, J., Haran, M., & Ferrari, M. (2017). An ensemble approach to predicting the impact of vaccination on rotavirus disease in Niger. *Vaccine*, 35 (43), 5835-584
- Pitzer, V. E., Patel, M. M., & Lopman, B. A. (2011). Modeling rotavirus strain dynamics in developed countries to understand the potential impact of vaccination on genotype distributions. *PNAS*. 108(48), 19353-19359. <https://doi.org/10.1073/pnas.1110507108>
- Pitzer, V. E., Atkins, K. E., De-Blasio, B. F., Van, T., Efferterre, Atchison, C. J., & Harris, J. P.(2012). Direct and indirect effects of rotavirus vaccination: comparing predictions from transmission dynamic models. *PLoS ONE*, 7 (8), e42320. <https://doi.org/10.1371/journal.pone.0042320>
- Shim, E., & Galvani, A. P. (2009). Impact of transmission dynamics on the cost-effectiveness of rotavirus vaccination, *Vaccine*, 27 (30), 4025-4030
- Sydney, Randall. (2023). How Serious Is Rotavirus? A Look at Worldwide Statistics, <https://www.healthline.com/health/rotavirus-season#fa-qs>
- White, L. J., Buttery, J., Cooper, B., Nokes, D. J., & Medley, G. F. (2008). Rotavirus within day care centres in Oxfordshire, UK: characterization of partial immunity. *Journal of the Royal Society Interface*, 5(29). <https://doi.org/10.1098/rsif.2008.0115>